EXPERIMENTAL TESTING TECHNIQUES TO DETERMINE UNREINFORCED MASONRY MATERIAL PROPERTIES

D.J. HEATH[1], E.F. GAD[2] AND J.L. WILSON[3]
THE UNIVERSITY OF MELBOURNE

AUTHORS:

[1] PhD Candidate, The University of Melbourne, Victoria, Australia

[2] Senior Research Fellow, The University of Melbourne, and Senior Lecturer, Swinburne University of Technology, Victoria, Australia

[3] Associate Professor, The University of Melbourne, Victoria, Australia

ABSTRACT:

A research project is currently in progress to investigate the response of residential structures to mining activities. Ground vibrations and airblast generated from mining activities predominantly cause racking and flexural response of houses. This article considers strength characteristics of both unreinforced brick masonry and common domestic tiles related to serviceability crack development. Various techniques are employed to determine the in-plane and out-of-plane strength of masonry. Common testing techniques that establish properties related to local and global behaviour and masonry properties from experimental investigations are presented. The data provides examples of brick masonry strength characteristics commonly found in Australian brick veneer construction. Data from bending tests conducted on two common types of tiles is also presented for comparison. Damage thresholds established using testing techniques discussed in this research will have direct applications to earthquake loading on residential structures.

1 - INTRODUCTION

In several locations around Australia mining and quarry activities that involve blasting are relatively close to residential areas. Disputes often arise between residents and operators regarding the effect of ground vibration on houses, particularly the reasons for cracking of non-structural components. Light-framed brick veneer construction is the most popular form of low-rise house construction in Australia. The two main non-structural components in this type of construction are brick-veneer cladding and plasterboard interior lining. An extensive research project is currently in progress to investigate the response of residential structures to low level vibrations. The project is focusing on non-structural damage such as crack initiation and development in plasterboard (Corvetti et al, 2003) and brick veneer walls which forms the focus of this paper.

A further development of this project will be to investigate crack initiation and propagation in perforated brick veneer walls when subjected to racking loads. Component and subassembly tests will be performed to determine material properties used as input for Finite Element Modelling to conduct a parametric study. Parameters to be considered include opening size and location, effect of returns, load combinations (e.g., settlement, racking and flexure) and influence of brick ties.

The response of brick-veneer walls to blast loading (ground vibration and air-blast) can be classified into flexural out-of-plane response and in-plane shear (racking) response. In order to assess the performance of brick veneer walls to blast loading, knowledge of masonry properties is required for both flexure and shear. Numerous methods to test the flexural strength exist, some of which are presented here. However, the in-plane shear response of masonry walls to ground vibrations is the main focus of this research. Both static and dynamic properties of masonry are required to model masonry walls subjected to blast vibrations and environmental effects. In addition to brick veneer, typical domestic ceramic tiles are briefly considered in this study. Failure stress and strain for these tiles have been experimental obtained and are outlined in this paper.

2 – FLEXURAL TESTING

Bending failure may occur either about a plane parallel to the bed joints, about a plane perpendicular to the bed joints, or both. There are two methods commonly employed to establish the flexural tensile strength of masonry. These are discussed below.

2.1 - Bond Wrench Test: The Australian Masonry Standard (AS 3700, 2001) Appendix D specifies that at least six tests must be performed on prisms containing between two and seven units, where the ASTM Standard Test Method for Measurement of Masonry Flexural Bond Strength (ASTM C 1072, 2000) specifies a *minimum* of two units.

The apparatus includes a wrench to apply a bending moment, a clamping mechanism to transfer the moment to the specimen and a supporting frame. The masonry prism is fastened vertically in the supporting frame. The lever arm length is not specified, and does not seem to have any discernable effect on the various strain gradients produced

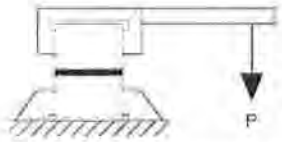

Figure 1: Bond Wrench

by different axial compression and bending ratios (Drysdale, et al., 1994). AS 3700, D6.4.1 specifies the uniform loading rate to be between 10kg/min and 15 kg/min. ASTM C 1072 specifies total load to be applied uniformly between one and three minutes duration.

The bond wrench test has been known to produce highly variable results. Variations in unit and mortar characteristics, workmanship, curing, etc, are all known to affect bond strength. McGinley (1993 and 1996) conducted an investigation into the validity of the bond wrench test procedure according to ASTM C 1072-86. An epoxy block was fabricated to represent a masonry couplet and instrumented with 16 strain gauges at the joint level. The use of separate bearing pads (similar to the AS 3700 procedure) in the upper and lower clamping devices was observed, rather than solid bearing plates. Good correlation was discovered between predicted and measured results at lower strain levels. At higher strain levels a non-linear strain distribution developed, suggesting one possible limitation of the AS 3700 bond wrench test. By substituting a solid bearing plate for the individual pads, a much closer measured strain to predicted strain was achieved. A second aspect of McGinley's research focused on the distance from the top of the bottom clamp to the point of strain measurement (mortar joint). This distance was increased from 12mm to 38mm resulting in a strain distribution much closer to being linear and equal to the predicted strain distribution. The AS 3700 25mm minimum distance specification lies in the middle of this range, suggesting potential for a non-linear strain distribution.

A third feature investigated by McGinley was varying the loading rate on concrete couplet specimens. Loading rates investigated were 130 N/min, 270 N/min and 400 N/min each on 20 specimens. The study found higher load rates may be responsible for an increase in flexural strength although the increase in strength was not consistent with loading rate. The results did reflect a higher coefficient of variation with higher loading rates. The second component of the study conducted by McGinley (1996) discovered different bond wrench testing apparatus are responsible for introducing variability into the bond wrench test results.

An investigation of masonry constructed under ordinary site control in the Melbourne-Geelong area by McNeilly et al (1996) discovered considerable variation in flexural tensile bond strength using the bond wrench test according to AS 3700. Half of the 25 samples tested had calculated characteristic bond strengths exceeding the AS 3700 0.2 MPa assumed strength, although small sample sizes were taken. Crude mortar batching procedures resulting in mortar composition variations from 1:0:4.2 (c:l:s) to 1:0:12.7 were thought to be largely responsible for the high variation (COV values from each site range from 0.15 to 0.52) in bond strength.

2.2 - Beam Test: An alternative procedure to the bond wrench test used to measure flexural bond strength is the beam test. When conducting the third point beam test in accordance with AS 3700 D7.1, a stack-bonded prism consisting of either seven or nine units is required. ASTM C 1390 also covers the third-point beam test. However, it specifies the prism should consist of either 4, 7, 10, 13 or 16 courses such that the aspect ratio exceeds 2.5. With the exception of loading rate, the remainder of this procedure is identical to that of AS 3700 D6.4.

Two steel supporting bars are used to support the prism. The load is applied through two bars on the upper surface. The load is applied equally between the two bars at a constant rate until failure (ASTM C 1390 specify the duration of this to be between one and three minutes). Harris (1990) compared the variability of results from the bond wrench and third-point loading method. The COV for the bond wrench test for all samples was 25.9%, where the COV for the third-point loading method was only 13.0% suggesting substantial improvements in uniformity of results. The average flexural bond strength of the 25 samples tested was found to be 0.53 MPa.

An alternative to the third-point beam test is the uniform loading method in accordance with ASTM C 1390. Minimum requirements for testing are five specimens and a height of five units or at least 460mm. Support conditions are identical to that of the AS 3700 third-point beam test. The application of a uniform load is achieved through an air bag in contact with the entire upper face area of the specimen. The load should increase uniformly at a rate such that the ultimate load is applied between one and three minutes from commencement of loading.

a) Third-Point Loading b) Uniform Loading

Figure 2:

Drysdale et al. (1994) notes a high scatter of characteristic tensile bond strengths in the uniform loading test could lead to high coefficients of variation if the minimum of five specimens are tested. It is also suggested that a low joint strength and high bending moment combination could bias the results since other joints with higher strengths aren't tested. Based upon previous research, Drysdale also states that the bond wrench test leads to higher mean flexural bond strengths as opposed to those obtained from the beam test methods. This view is also supported by Harris who refers to the influence of the compressive stress component of the bond wrench test.

3 – SHEAR TESTING

Numerous methods have been developed to measure the shear capacity of masonry. AS 3700 Cl. 3.3.4 allows the characteristic shear strength of masonry, f'_{ms}, to be taken as the lesser of $1.25f'_{mt}$ or 0.35 MPa, where f'_{mt} is the characteristic tensile strength of masonry. It does not specify a test procedure to investigate masonry shear strength. It expresses the shear strength using the Coulomb friction relationship; $V_d = V_o + V_f$. Here, V_o represents the shear bond strength and V_f represents the shear friction strength. (This is commonly expressed as $\tau = \tau_o + \mu\sigma$, where τ = shear strength, τ_o = shear bond strength, μ = coefficient of friction and σ = stress normal to bed joint.) Five commonly used procedures used to quantify V_o and V_f are presented in this section and the advantages and disadvantages of each are discussed. The first three procedures investigate the shear strength at the unit/mortar interface whilst the remaining two procedures investigate the shear strength at a system level.

*3.1 - **Couplet Test:*** Two bricks separated by mortar are loaded to develop shear stress as shown in Figure 3a. This minimises bending stresses and ensures the resultant force acts through the mortar joint. However, loads are applied to the brick specimens that divert the compressive stresses to the mortar joint. Rots et al. (1997) report this test method has potential to cause peak normal and shear stresses that could be three times greater than the average shear stresses occurring in the joint. Precompression normal to the bed joints may also be applied using hydraulic jacks and springs.

*3.2 - **Modified Couplet Test:*** Rots et al developed a test as an alternative to the preceding couplet (and triplet) test to determine the shear strength of a mortar bed. An important improvement of this procedure is the stiff steel blocks diverting the load rather than the load diversion occurring through the specimen as shown in Figure 3b. Jacking screws apply compressive stress to the mortar joint and shear forces to the metal blocks. A loading rate of 2mm/hour was reported by both Rots et al. (1997) and Hansen (1999).

*3.3 - **Triplet Test:*** This test comprises three brick units and two mortar joints. Figure 3c depicts a typical set-up. This is the shear bond test prescribed by Eurocode 6 (1996). Shear transfer occurs on either side of the middle brick, thus complex fixtures required to ensure uniform stress distribution across each mortar bed are not required. Without precompression the cohesion, τ_o, of the mortar joint may be determined. If precompression is included, the friction coefficient, μ, may be found.

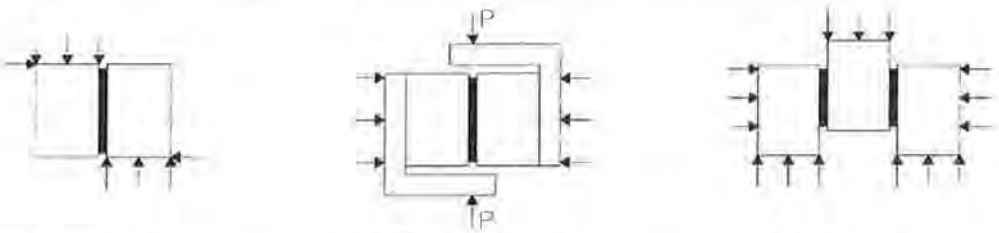

a) Couplet test **b)** Modified Couplet **c)** Triplet

Figure 3:

Beattie et al. (2001) investigated the bond strength of masonry under dynamic loading conditions using a drop hammer (triplet) test rig. The dynamic shear strength was similar to the static shear strength up to a loading rate of 47 MPa per second. Beyond this the dynamic shear strength increased markedly.

*3.4 - **Diagonal Tension Test:*** The diagonal tension test is intended to replicate the behaviour of a full wall panel experiencing shear. The ASTM test method for diagonal tension in masonry assemblages (ASTM E 519, 2002) requires a minimum of three 1.2m x 1.2m masonry wallettes to be loaded through steel shoes on the diagonal for this test as shown in Figure 4. Compressometers and extensometers are used to measure strain. The first half of the ultimate load may be applied at a convenient rate. The second half must be applied at a uniform rate such that the ultimate load is achieved in one to two minutes duration.

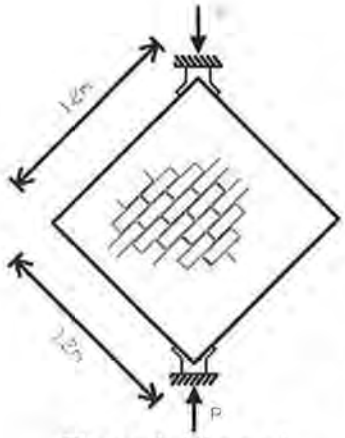

Figure 4: Diagonal Tension Test

Drysdale et al. (1994) comments that due to resultant stress fields, this test may favour a line for crack growth that doesn't follow the path of least resistance. It is also suggested that the loading shoes could assist the development of a compression strut and hence an ultimate load greater than that required to produce tension cracks.

A study conducted by Lissel et al. (2000) into the shear strength of masonry wallettes discovered a significant reduction in variation of results with increased precompression in the diagonal tension test. At zero precompression the COV was 36.0 but reduced to 10.8 at a precompression of 1.5 MPa. The mean strength of specimens at 0, 0.75 and 1.5 MPa were 158, 253 and 335 kN, respectively.

3.5 - Racking Test: An alternative to the diagonal tension test is the racking test as described in ASTM E 72 (2002). This procedure requires a minimum of three specimens, each with dimensions of 2.4m x 2.4m. A hold-down tie is attached to prevent uplift and a timber beam attached to the top of the specimen to evenly distribute the racking load. A point load is applied in a compressive manner to the beam when the test is carried out. The load is to be applied at a uniform rate to increments, displacements measured and then released. The intervals are 0-3.5 kN, 0 – 7.0 kN and 0 – 10.5 kN. The recommended loading rate is to be at least 3.5 kN in a two minute period. After the specimen has been loaded to 10.5 kN, the load is to be increased until failure of the panel results.

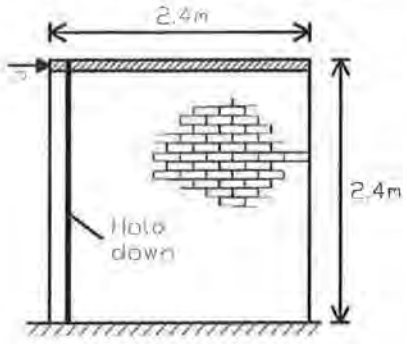

Figure 5: Racking Test

One criticism of the racking test is that the hold-down introduces compressive stresses that cannot be measured, potentially increasing the shear resistance.

4 – CERAMIC TILE TESTS

Bending tests were conducted on typical ceramic tiles used in Australian residential construction. Specimens included Johnson tiles (10 specimens) and Cotto tiles (8 specimens). Each specimen was simply supported with a line load applied at mid-span as shown in Figure 6. A loading rate of 2mm/min was applied until half the ultimate load was achieved. The loading rate was then reduced to 0.5mm/min until failure. Perfectly elastic behaviour was observed with each specimen exhibiting brittle failure. The results of these tests are summarised in Table 1 below. Some tiles were required to be cut due to the test apparatus limiting specimen width to 100mm.

Figure 6: Bending test on tile

Brand	Density (kg/m^3)	Ultimate Flexural Strength			Failure Flexural Strain		
		Average (MPa)	St. Dev (MPa)	COV (%)	Average ($\mu\varepsilon$)	St. Dev ($\mu\varepsilon$)	COV (%)
Johnson	1756	22.2	3.9	17.6	940.9	152.3	16.2
Cotto	2150	35.7	4.1	11.5	910.3	79.2	8.7

Table 1: Results from mid-point bending tests on ceramic tiles

The Cotto tile was found to have an average Young's Modulus of 39.2 GPa compared with 23.6 GPa for the Johnson tile, reflecting a higher flexural rigidity.

5 - CONCLUSION

A number of techniques to establish properties of masonry have been discussed, highlighting important factors for consideration when analysing results. The outcomes from this ongoing research will have direct benefits to earthquake engineering insurance related issues.

The bond wrench, third-point loading and uniform loading beam tests are all commonly used techniques to establish the flexural moment of resistance of masonry. The bond wrench test may overestimate flexural strength and has historically produced results of high variability. The third-point loading test seems to be the optimal procedure since the uniform loading beam test has the potential to bias results.

The couplet test establishes the shear strength of the unit/mortar joint but has potential to introduce peak normal and shear stresses. This deficiency led to the development of the modified couplet test. A third method for testing shear strength is the triplet test. Data presented form this test suggests a threshold exists above which the shear strength of masonry increases when subjected to dynamic loading. Larger scale tests used to measure the shear strength of masonry are the diagonal tension and racking test. The diagonal tension test is useful to replicate full wall behaviour but may overestimate shear strength. The racking test offers a procedure to test a complete wall with some uncertainty introduced from the use of a hold-down.

From the study, it is recommended that the modified couplet will be used to evaluate the unit/mortar interface shear strength, whilst either of the two global shear tests could be used to investigate shear effects in wall systems.

Ultimate flexural tensile strength and failure strains were obtained experimentally for common Australian domestic tiles.

ACKNOWLEDGEMENTS

This research is funded by an ARC Linkage Grant No. LP0211407. The authors would like to acknowledge input and contribution of the research partners Mr. Alan Richards and Adrian Moore of Terrock Pty Ltd.

REFERENCES

AS 3700 – 2001, Masonry Structures, Standards Australia International Ltd

ASTM E 72 – 02, Standard Test Methods of Conducting Strength Tests of Panels for Building Construction, ASTM International

ASTM E 518 – 02, Standard Test Methods for Flexural Bond Strength of Masonry, ASTM International

ASTM E 519 – 02, Standard Test Method for Diagonal Tension (Shear) in Masonry Assemblages, ASTM International

ASTM C 1072 – 00a, Standard Test Method for Measurement of Masonry Flexural Bond Strength, ASTM International

Beattie, G., Molyneaux, T.C.K., Gilbert, M. and Burnett, S., Masonry Shear Strength Under Impact Loading, 9th Canadian Masonry Symposium, Canada, 4-6 June, 2001

Corvetti, J., Gad, E.F., Deiss, M. and Wilson, J.L., Estimation of Non-Structural Damage in Light Framed Residential Structures, Proceedings of the Annual Australian Earthquake Engineering Society (AEES) Conference, Melbourne, Australia, 2003

Drysdale, R.G., Hamid, A.A. and Baker, L.R., Masonry Structures: Behaviour and Design, Prentice Hall, New Jersey, 1994

Eurocode 6: Design of Masonry Structures, Part 1.1. General rules for buildings – Rules for reinforced and unreinforced masonry. (1996)

Hansen, K.F., Bending and Shear Tests with Masonry, Danish Building Research Institute, SBI Bulletin 123, 1999

Harris, H.A., Proposed Revisions to the Masonry Flexural Bond Strength Procedure, Proceedings of the Fifth North American Masonry Conference, Urbana-Champaign, 3-6 June, 1990, pp. 687 – 700.

Lissel, S.L., Simundic, G., Page, A.W. and Shrive, N.G., Improving the Shear Resistance of Masonry, 12th International Brick/Block Masonry Conference, Spain, 25-28 June, 2000

McGinley, W.M., Flexural Bond Strength Testing – An Evaluation of the Bond Wrench Testing Procedures, Masonry: Design and Construction, Problems and Repair, ASTM STP 1180, American Society for Testing and Materials, Philadelphia, 1993, pp. 213 - 227

McGinley, W.M., An Evaluation of Bond Wrench Testing Apparatuses, Masonry: Esthetics, Engineering, and Economy, ASTM STP 1246, American Society for Testing and Materials, 1996, pp. 100 – 115

McNeilly, T., Scrivener, J., Lawrence, S. and Zsembery, S., A Site Survey of Masonry Bond Strength, Australian Civil/Structural Engineering Transactions, Vol. CE38, No. 2, 3 & 4, 1996, pp. 103 – 109

Rots, J.G., Pluijm, R. v.d., Vermeltfoort, A.Th. and Janssen, H.J.M., Structural Masonry, A.A. Balkema, Netherlands, 1997

Seisun, M., Parsanejad, S. and Jankulovski, E., Experimental Behaviour of Clay Brick Masonry Subject to Compression and Shear, Australasian Structural Engineering Conference, Sydney, 21-23 September, 1994, pp. 691-695

A RELATIVE SEISMIC VULNERABILITY ANALYSIS OF HERVEY BAY CITY, QUEENSLAND.

MIKE TURNBULL
FACULTY OF INFORMATICS AND COMMUNICATIONS
CENTRAL QUEENSLAND UNIVERSITY, BUNDABERG

JOHN FICHERA
FACULTY OF ENGINEERING AND PHYSICAL SCIENCES
CENTRAL QUEENSLAND UNIVERSITY

AUTHORS:

Mike Turnbull received his bachelor degree in physics and mathematics from QUT, with distinctions, in 1992. He currently teaches C++ and Java at the Bundaberg Campus of Central Queensland University (CQU). He completed a Master of Applied Science Degree by research and thesis at CQU in 2002. The title of his master's thesis was A Seismic Hazard Assessment and Microzonation of Bundaberg.

Email: M.Turnbull@cqu.edu.au

John Fichera received his bachelor degree in science (Applied Physics) from CQU, with distinction, in 1998. He has recently completed an applied physics honours program at CQU. As part of his honours project John is participating in a seismic shaking vulnerability survey of the Hervey Bay city area, using a methodology developed by Mike Turnbull.

ABSTRACT

Ground velocity microseismograms have been collected from 347 test sites within the Bundaberg, Burnett Shire, and Hervey Bay areas. Spectral ratios have been calculated for those sites using the Nakamura technique and seismic shaking vulnerability microzonations have been carried out. The results can be used to supplement the general recommendations given in Australian Standard AS 1170.4-1993 for earthquake loadings within the city.

The Hervey Bay microzonation is presented both as a stand-alone analysis of the relative vulnerability between adjacent zones within the immediate test area, and as a comparison of the relative vulnerability between Hervey Bay and Bundaberg/Burnett.

1. Introduction

One of the authors (Turnbull, 2001) has previously presented an earthquake shaking vulnerability microzonation survey methodology based on an analysis of Nakamura Spectral Ratios (NSRs) (Nakamura, 1989) obtained from velocity seismograms of ambient ground motion recorded at test sites throughout the area of interest. The results of the methodology can be used in a GIS to display the relative vulnerability zones as colour coded maps. Partial surveys of Bundaberg (Turnbull 2000 & 2001), Burnett Shire East (Turnbull 2003), and Hervey Bay (Fichera 2003) have been conducted. The extensibility of the methodology has been tested by successfully combining datasets from physically contiguous test areas (Bundaberg and Burnet Shire East)(Turnbull 2003).

The microzonation surveys discussed in this paper were conducted using the methodology described in Turnbulls previous work (Turnbull, 2000, 2001, 2003). In this paper the ability of the methodology to combine datasets from non-contiguous test areas is demonstrated. The combined Bundaberg/Burnett Shire East and the Hervey Bay results are presented as internal, stand-alone surveys, and then as comparative surveys relative to one another.

2. Bundaberg/Burnett East Internal Survey

The dataset used for the Bundaberg/Burnett East internal survey consisted of 118 Bundaberg sites and 152 Burnett sites. The combined dataset of 270 sites was analysed to define relative shaking vulnerability values for each site, and for three categories of structure; namely low rise, medium rise and high rise.

Figures 1a, 1b and 1c show the mapped results. The lighter shaded zones represent the lowest relative vulnerability, ranging in five values through to the highest relative vulnerability zones in the darker shades. The test sites are shown as white dots. The statistical proportions of vulnerability ratings are graphed in Figure 3a.

It is noted that the sites of highest relative vulnerability for all structure categories correspond to the sedimentary areas at the mouths of the Burnett and Elliott rivers. In the low rise category this high risk vulnerability is extended to a swampy area on the main arterial road linking Bundaberg and Bargara. In the low rise category there is a corridor of relatively high risk trending from Burnett Heads in the north, to the south through sparsely populated farming areas. For all three structure categories broad areas of moderately low vulnerability are indicated, and, unlike the Hervey Bay area, isolated zones of low relative vulnerability are apparent.

It should also be noted that, as there were very few test sites to the northwest of the Burnett River, the relative vulnerability in that section of all maps shown in this paper has been disregarded as an artefact of the GIS's IDW raster production process.

3. Hervey Bay Internal Survey

The dataset for the Hervey Bay internal survey consisted of 77 test sites in the urbanised area of the Hervey Bay Shire. Figures 2a, 2b and 2c show the results side-by-side with

the Bundaberg/Burnett East internal survey maps. The statistical proportions of vulnerability ratings are graphed in Figure 3b.

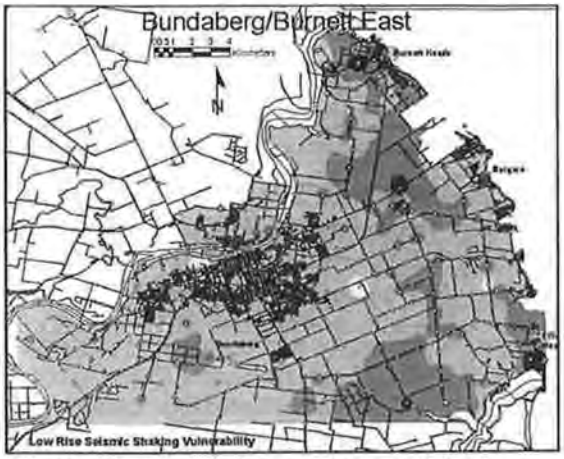

Figure 1a: Bundaberg/Burnett East
Low rise internal microzonation

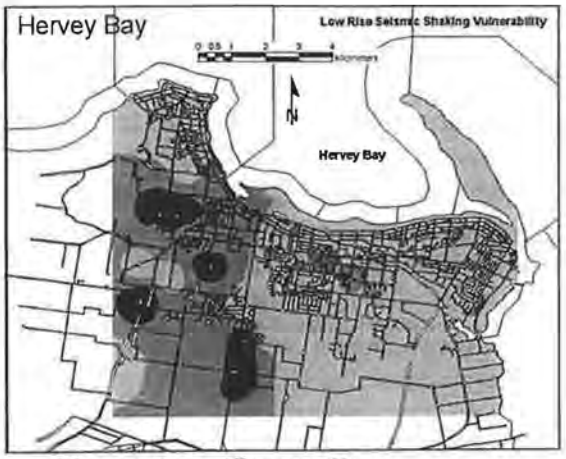

Figure 2a: Hervey Bay
Low rise internal microzonation

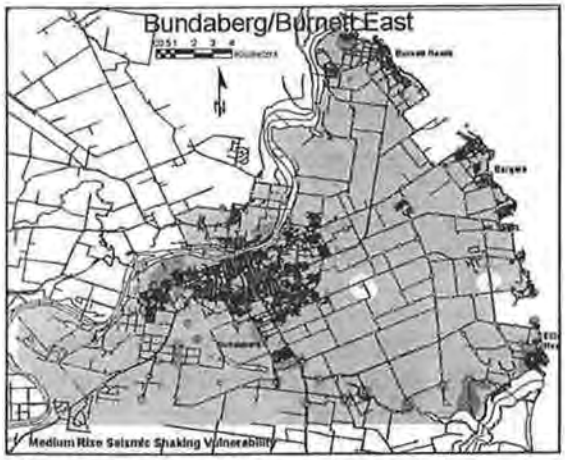

Figure 1b: Bundaberg/Burnett East
Medium rise internal microzonation

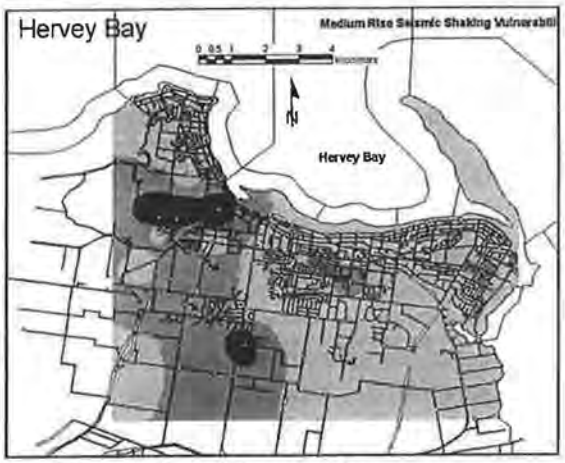

Figure 2b: Hervey Bay
Medium rise internal microzonation

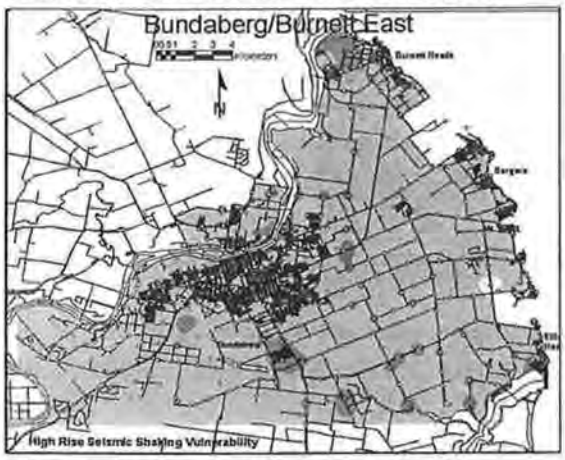

Figure 1c: Bundaberg/Burnett East
High rise internal microzonation

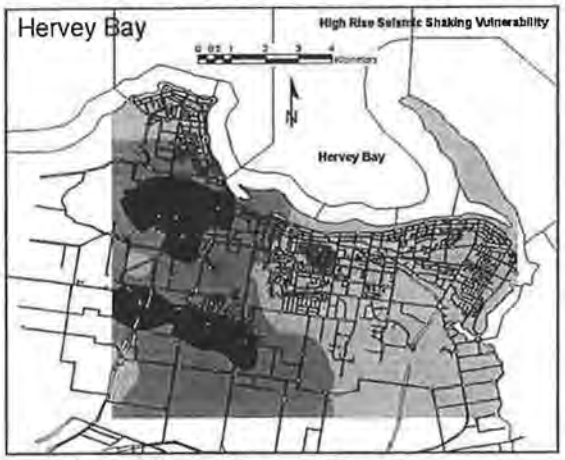

Figure 2c: Hervey Bay
High rise internal microzonation

It is noted that in Hervey Bay, for all structure categories, whilst there are apparent areas of moderately low relative vulnerability, particularly in the eastern two thirds of the test area, the western third of the test area displays noticeably high relative vulnerability. This high relative vulnerability area forms a fan, radiating from a small coastal inlet and extending to the west and south. This area includes the main arterial road that provides access to Hervey Bay from Maryborough and other centres. It is also noted that, unlike the Bundaberg/Burnett East internal survey, no zones of the lowest relative vulnerability have been identified.

4. Statistical Comparison of Internal Vulnerabilities

Figure 3 provides a graphical representation of the internal vulnerability of both the Bundaberg/Burnett East, and the Hervey Bay areas. The vulnerability is displayed as the proportional frequency of the relative vulnerability ratings, within each test area, based on the dataset obtained from within that test area. The graphs show that the Hervey Bay area exhibits a higher internal relative vulnerability regime than the Bundaberg/Burnett area, particularly for high rise structures.

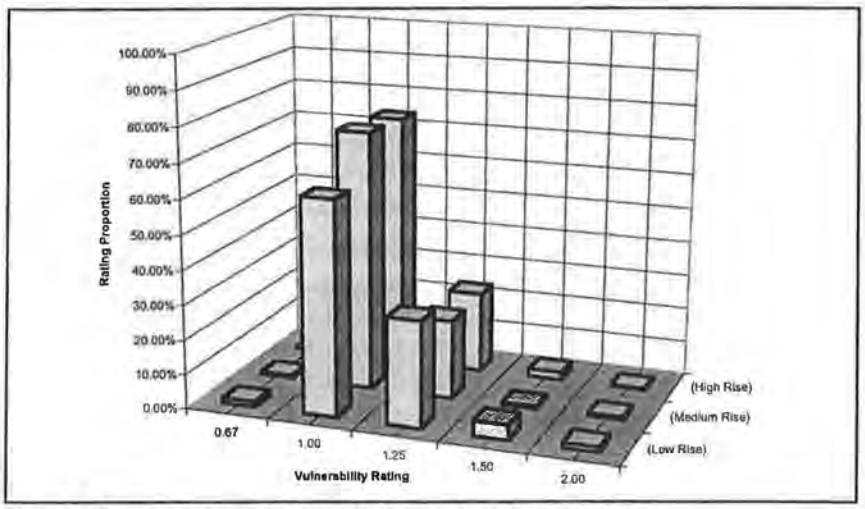

Figure 3a: Bundaberg/Burnett East Internal vulnerability

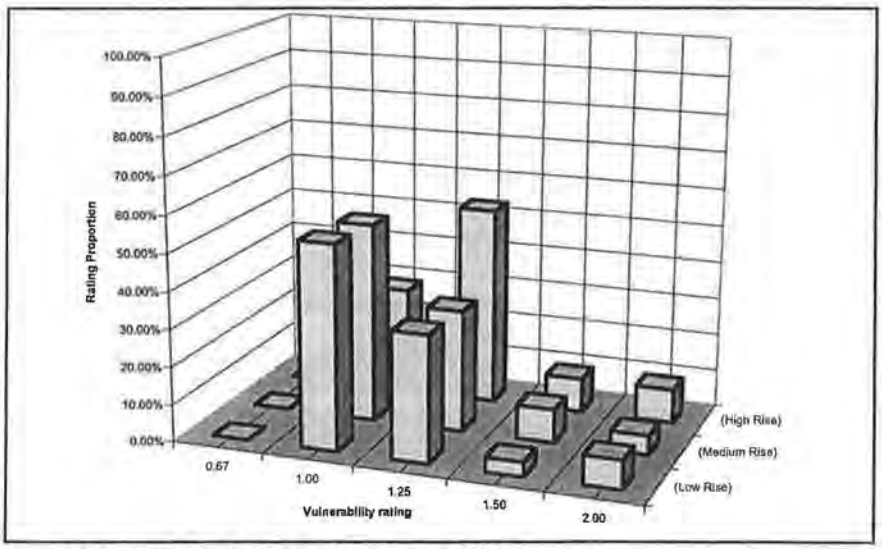

Figure 3b: Hervey Bay Internal vulnerability

5. Bundaberg/Burnett East Hervey Bay Comparative Survey

The dataset for the Bundaberg/Burnett East Hervey Bay comparative survey consisted of that obtained from combining all 347 test sites. Figures 5 and 6, a, b and c show the results indicated by the Bundaberg/Burnett East, and the Hervey Bay comparative survey maps. The statistical proportions of the comparative vulnerability ratings are graphed in Figures 4a and 4b. The results indicate that the Hervey Bay area contains a marginally larger proportion of relatively high vulnerability sites in the low rise and medium rise categories than the Bundaberg/Burnett East area, but a slightly lower proportion in the high rise category. The comparative vulnerability regime for the Bundaberg/Burnett East area is little changed from its internal regime. However the comparative regime of the Hervey Bay area is significantly different to its internal regime, having shifted toward a lower relative vulnerability, particularly in the high rise category.

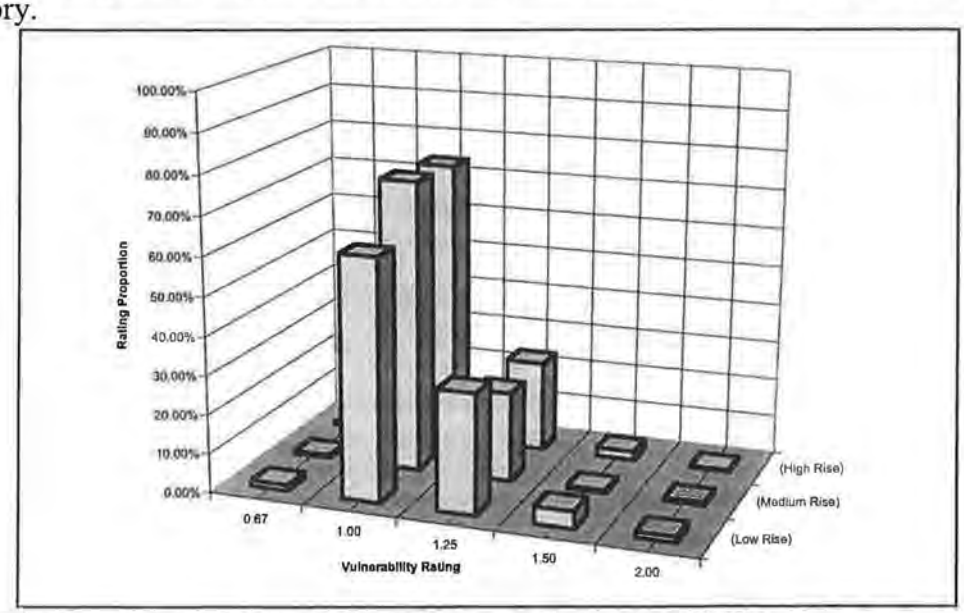

Figure 4a: Bundaberg/Burnett East Comparative vulnerability

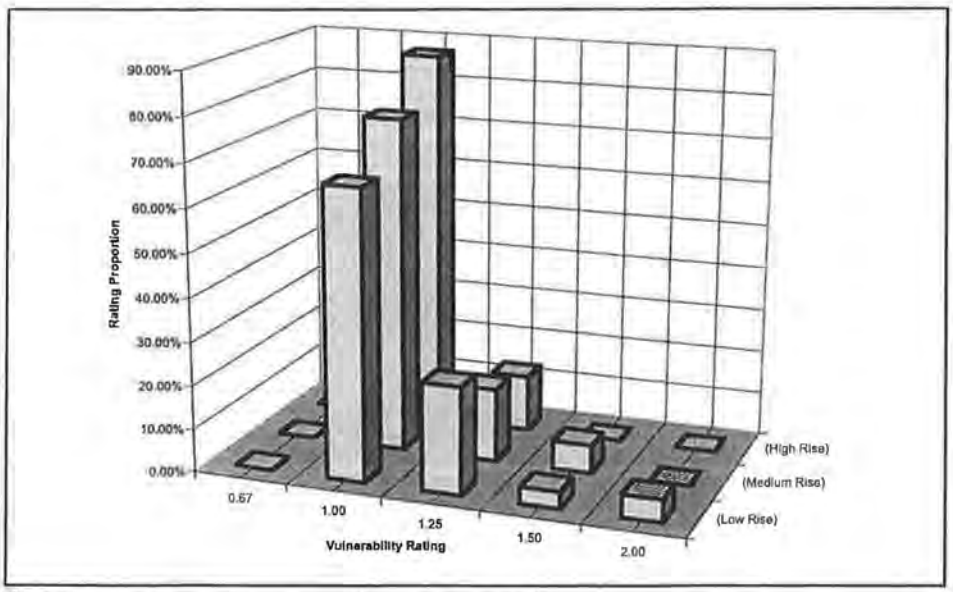

Figure 4b: Hervey Bay Comparative vulnerability

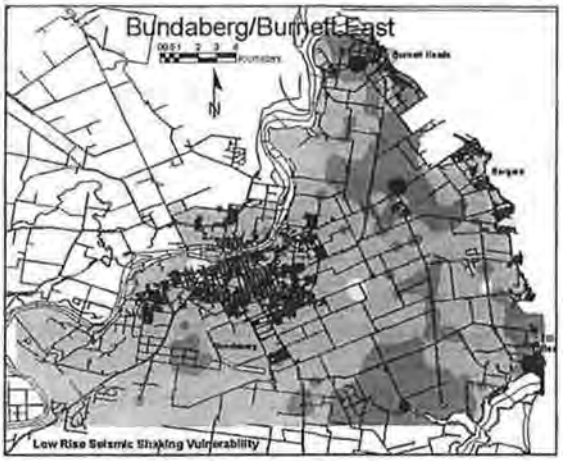

Figure 5a: Bundaberg/Burnett East
Low rise comparative microzonation

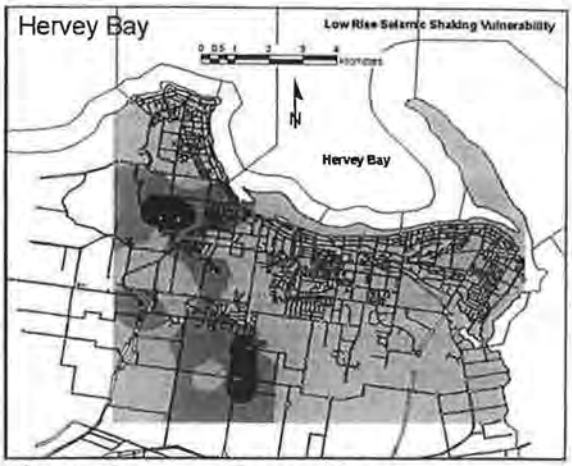

Figure 6a: Hervey Bay
Low rise comparative microzonation

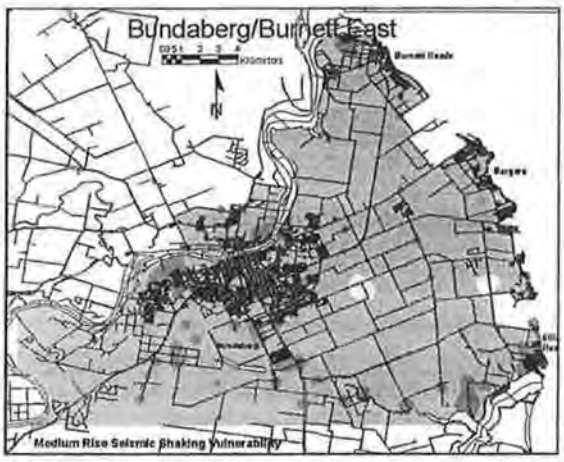

Figure 5b: Bundaberg/Burnett East
Medium rise comparative microzonation

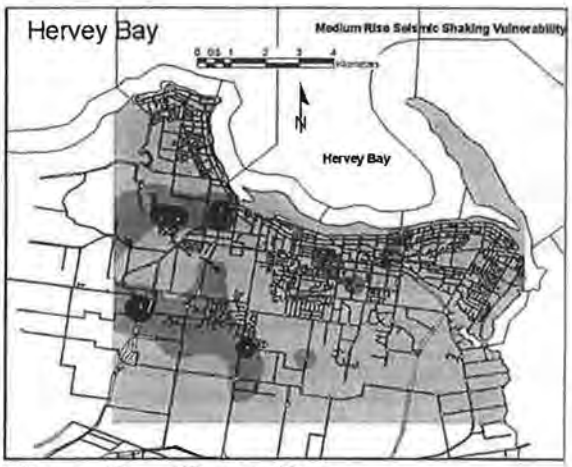

Figure 6b: Hervey Bay
Medium rise comparative microzonation

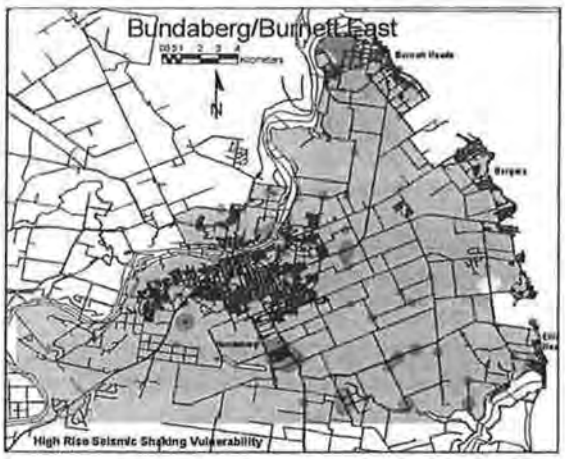

Figure 5c: Bundaberg/Burnett East
High rise comparative microzonation

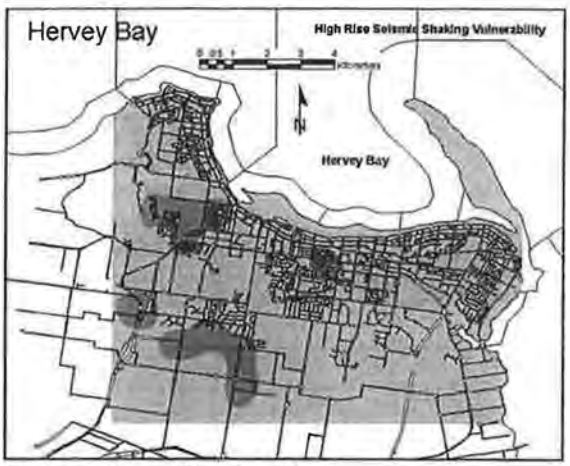

Figure 6c: Hervey Bay
High rise comparative microzonation

6. Conclusion

The consistency of the results produced by the internal and comparative surveys demonstrates the extensibility of the methodology. As the size of the dataset grows, encompassing both contiguous and distant physical test areas, different zones within the dataset can be compared as to their relative shaking vulnerability. Moreover, the increase in microzonation detail evident in the Hervey Bay internal survey, over the reduced detail in the Hervey Bay comparative survey, demonstrates that as the analysis dataset is increased, local detail is diluted, and as the analysis dataset is restricted, detail is enhanced.

This result is consistent with previous findings (Turnbull 2003) showing that the methodology is capable of eliciting internal detail by restricting the size of the dataset to the immediate region of interest.

7. Future Work

Figures 1 and 5 highlight the need to extend the Burnett Shire survey to include test sites to the northwest of the Burnett River, and to the south-western sector of the map. This will give full survey coverage for the extent of the map.

The current locations of low, medium and high rise structures within the survey areas also need to be mapped so that at risk structures can be identified.

8. References

Fichera J., (2003). *Microzonation of Hervey Bay*, Central Queensland University, Physics Honours Degree Project Report.

Nakamura, Y., (1989). *A Method for Dynamic Characteristics Estimation of Subsurface using Microtremor on the Ground Surface.* Quarterly Report of Railway Technical Research Institute Vol. 30, No. 1, pp. 25-33, February 1989.

Standards Association of Australia 1993. AS 1170.4 – (1993), *Minimum design loads on structures (known as the SAA Loading Code) Part4: Earthquake loads.* Standards Australia. ISBN 0-7262-8297

Turnbull, M.L., (2000). *Seismic Microzonation of Bundaberg, Queensland.* Proceedings of the Australian Earthquake Engineering Society Annual Conference, Hobart, Nov. 2000.

Turnbull, M.L., (2001). *A seismic assessment and microzonation of Bundaberg.* Central Queensland University, Masters Degree Thesis. Available online at http://www.infocom.cqu.edu.au/Staff/Mike_Turnbull/Publications/BundyMZ.pdf

Turnbull M.L., (2003). *Testing the Extensibility of an Earthquake Vulnerability Microzonation Methodology by Application at Bargara, Queensland.* 2003 Pacific Conference on Earthquake Engineering, Paper 10, Christchurch, New Zealand.

RISKS FROM THE RESPONSE OF NON-STRUCTURAL COMPONENTS TO SEISMIC LOADS IN BUILDINGS

HAIDER AL ABADI, EMAD GAD, NELSON LAM AND ADRIAN CHANDLER
THE UNIVERSITY OF MELBOURNE AND HONG KONG UNIVERSITY

AUTHORS:

Haider Al Abadi is a PhD student in the Department of Civil and Environmental Engineering, University of Melbourne

Emad Gad is Senior Research Fellow, University of Melbourne and Senior Lecturer, Swinburne University of Technology.

Nelson Lam is a Senior Lecturer in the Department of Civil and Environmental Engineering, University of Melbourne

Adrian Chandler is Professor, Department of Civil Engineering, Hong Kong University.

ABSTRACT:

See over

Risks from the response of non-structural components to seismic loads in buildings

Haider A. Al Abadi[1], Emad F. Gad[2], Nelson T. K. Lam[3] and Adrian M. Chandler[4]

1. PhD student, Department of Civil and Environmental Engineering, University of Melbourne.
2. Senior Research Fellow, University of Melbourne and Senior Lecturer, Swinburne University of Technology.
3. Senior Lecturer, Department of Civil and Environmental Engineering, University of Melbourne.
4. Professor, Department of Civil Engineering, Hong Kong University.

Abstract

This paper addresses the risks of failure of non-structural components (NSC) in buildings in future earthquakes. Non-structural components are classified into (I) mechanical components (e.g. boilers, tanks, pumps, and HVAC equipment), (II) Electrical and electronic components (e.g. transformers, generators, switchboards, computer networks, telecommunication systems and other electronic components) and (III) Architectural components (e.g. exterior curtain walls and cladding, non-loading bearing partitions, ceiling systems and ornaments such as marquees and signs). Failures of NSC could have severe life-safety and economic consequences which include damage caused by the overturning and falling of objects, and the loss of continuous functioning of key facilities. Floor-mounted or freestanding components with behaviour sensitive to the floor motions are of particular interest in this paper. Thus, damage to components resulted from inter-story drifts are outside the scope of the discussions.

This paper presents results of a recent field survey conducted by the authors on a range of building facilities in the Melbourne Metropolitan area. The survey highlights the fact that many critical NSC are potentially vulnerable to seismically induced damage due to the general lack of restraints. Simple analytical tools have been developed for the vulnerability assessment of the NSC, which are at risk. The assessment involves modelling the floor motions in terms of its peak response acceleration, velocity and displacements for any given earthquake motion affecting the building. This broadband approach to modelling is an innovative departure from the conventional approach of merely addressing accelerations. This paper also provides a brief description of a planned shaker-table testing program for studying the fragility of some floor-mounted components.

Introduction

Non-structural components (NSC) represent a high percentage of the total capital investment in the majority of buildings. Failure or damage to these components in an earthquake could disrupt the continuous functioning of a building and subject its occupants to significant risks. In buildings, NSC could generally be divided into (I) mechanical components, (II) electrical and electronic components, and (III) architectural components. Mechanical components include boilers, tanks, pumps and

HVAC equipments. Electrical and electronic components include transformers, generators, switchboards and telecommunication systems. Architectural components include items such as exterior curtain walls and cladding, non-load bearing partitions, ceiling systems, and ornaments such as marquees and signs. With a growing trend to "paperless offices" or "e-offices", the seismic protection of computer hardware deserves priority attention.

Figure 1. Rooftop tank failure, 1994 Northridge earthquake

This research is mainly concerned with roof/floor-mounted equipment, which are typically mechanical, electrical or electronic components. The motion sensitive behaviour of these components is central to the interests in this investigation. Components that are sensitive to inter-story drifts such as full-height partitions and vertical piping are outside the scope of discussions in view of the length limitations of the paper.

The vulnerability of non-structural components is well illustrated in recent experience from major earthquakes worldwide (Hall 1995, Phan and Tylor, 1996, and Naeim, 1999). An example of the failure of a typical roof-mounted component is shown in Fig.1 (Naeim 2001). Cost statistics on seismically induced non-structural damage are scarce. However, reports from reliable sources indicate that the economic costs of nonstructural damage generally well exceed those of structural damage in recent earthquake events (e.g. Brunsdon, 2001). The survey of 355 high-rise buildings by Arnold (1987) following the 1971 San Fernando earthquakes shows that 79% of the damage bill was associated with the failures of non-structural components. It has also been found that serviceability failures of building components could create havoc in terms of deaths and injuries. Lifeline facilities such as hospitals are generally exposed to higher consequence failures (Monto et al, 1996). Non-structural components in low and moderate seismic regions are particularly vulnerable due to the lack of restraints and suitable detailing.

To mitigate the potential risks to high consequence damage, it is important to envisage possible damage scenarios and accurately identify the types of existing components that require retrofitting in averting the damage. To fulfil this research objective, the investigation is divided in to following phases:

- Phase 1: Field surveys of a range of NSC commonly found in buildings and hospital facilities in the Melbourne Metropolitan Area.
- Phase 2: Broadband modelling of the seismically induced motions on the building floor at different levels in the building.
- Phase 3: Studies into the dynamic behaviour of representative NSC models based on both analytical modelling and shaker-table testings. The behaviour of components in sliding, rocking and overturning in partially restrained and unrestrained conditions will be examined in detail.
- Phase 4: Development of a practical and reliable scanning process which could accurately identify components which require retrofitting.

Field Survey of NSC in Melbourne

Field surveys of existing NSC had been conducted on a range of facilities including hospitals, office blocks and buildings for educational purposes. The survey reveals a general lack of restraints in roof/floor-mounted components, which include critical equipment. Some equipment are merely freestanding and hence could be subject to sliding, rocking, overturning or pounding when the building floor is in motion. Photos taken from field surveys (see the left hand half of Fig. 2) reveal the absence or lack of restraints of the components. Shown alongside the surveyed photos are recommendations by a Canadian organization for suitable retrofitting measures (*www.terrafirm.ca/sitemap.htm*). The comparison reveals a major vulnerability problem that has resulted from current local practices.

Retrofitting every NSC in all building facilities is clearly prohibitively costly and hence not feasible to implement. Thus, the research is targeted at modelling vulnerability accurately in order that limited resources could be directed effectively to avert potential high-consequence failures. Analytical and experimental investigations for accomplishing this key objective are outlined in the rest of the paper.

Proposed Analytical Method

The seismic evaluation of a component should be based on pre-defined objectives. Basic safety objectives would often be satisfied if the component does not slide or overturn in an earthquake. However, the component (e.g. computer/telecommunication equipment, transformers and generators), or a system, would need to function continuously in order to satisfy the "Immediate Occupancy Objectives". Thorough analysis or shaker-table testing could be required to ensure that certain high performance objectives are satisfied with the prescribed level of ground shaking. The analytical procedure for the vulnerability modelling of NSC is presented schematically in Figure 3.

The motions of the building floor would need to be modelled accurately in order that seismic actions on the components could be ascertained. Similar seismic performance levels apply to both the building structure and the non-structural components that are housed in the building. In the investigation, a range of building structures has been subject to time-history analyses.

Non-structural components would respond differently to the floor motion depending on a number of factors including the component dimensions (see Figure 4), weight and flexibility of the supports.

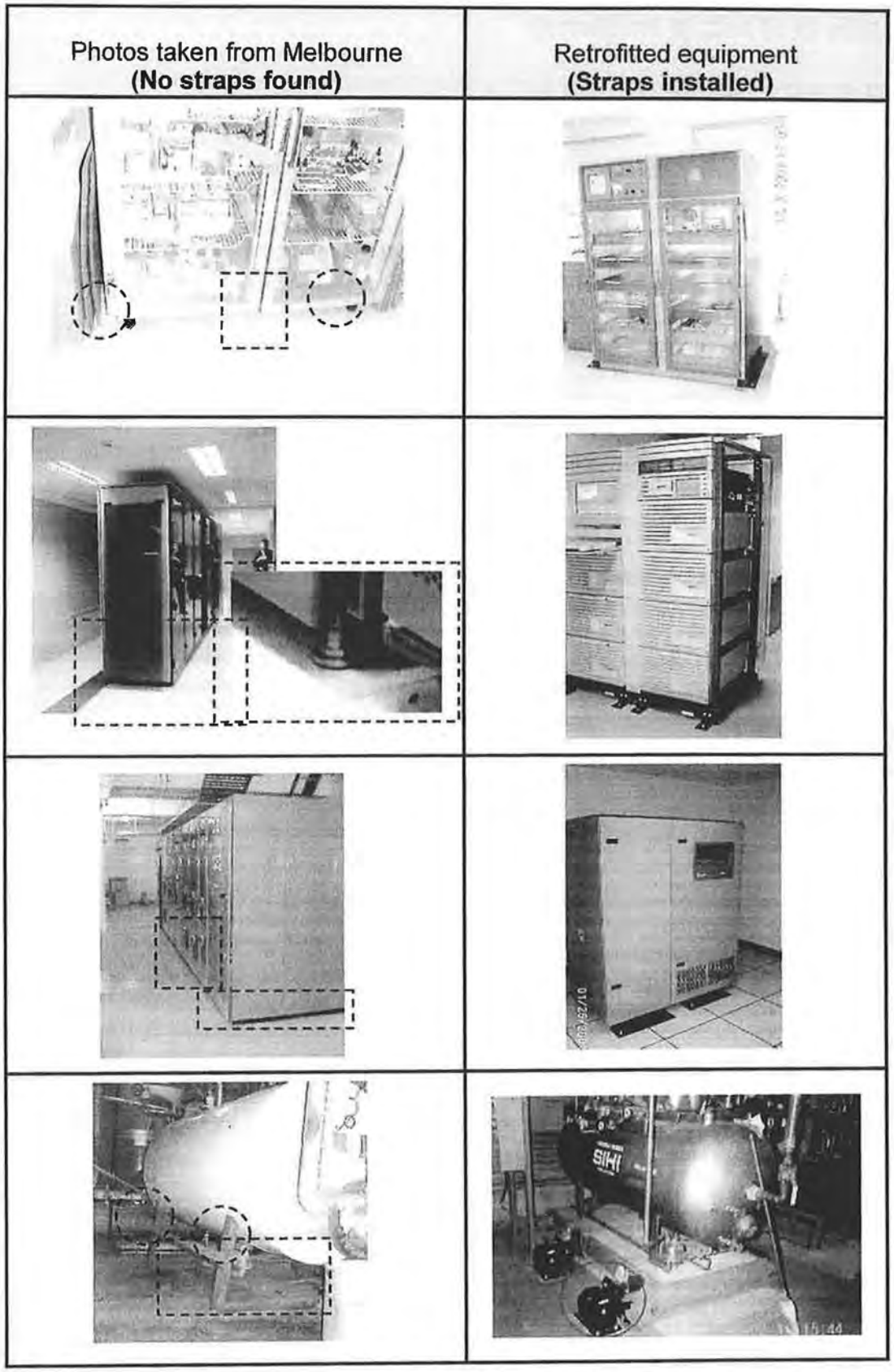

Figure 2 Photos of equipment from local surveys (left) and of equipment with supplementary restraints (right). (Photos of equipment with supplementary restraints have been reproduced with permission from Terra Firm Earthquake Preparedness Inc.)

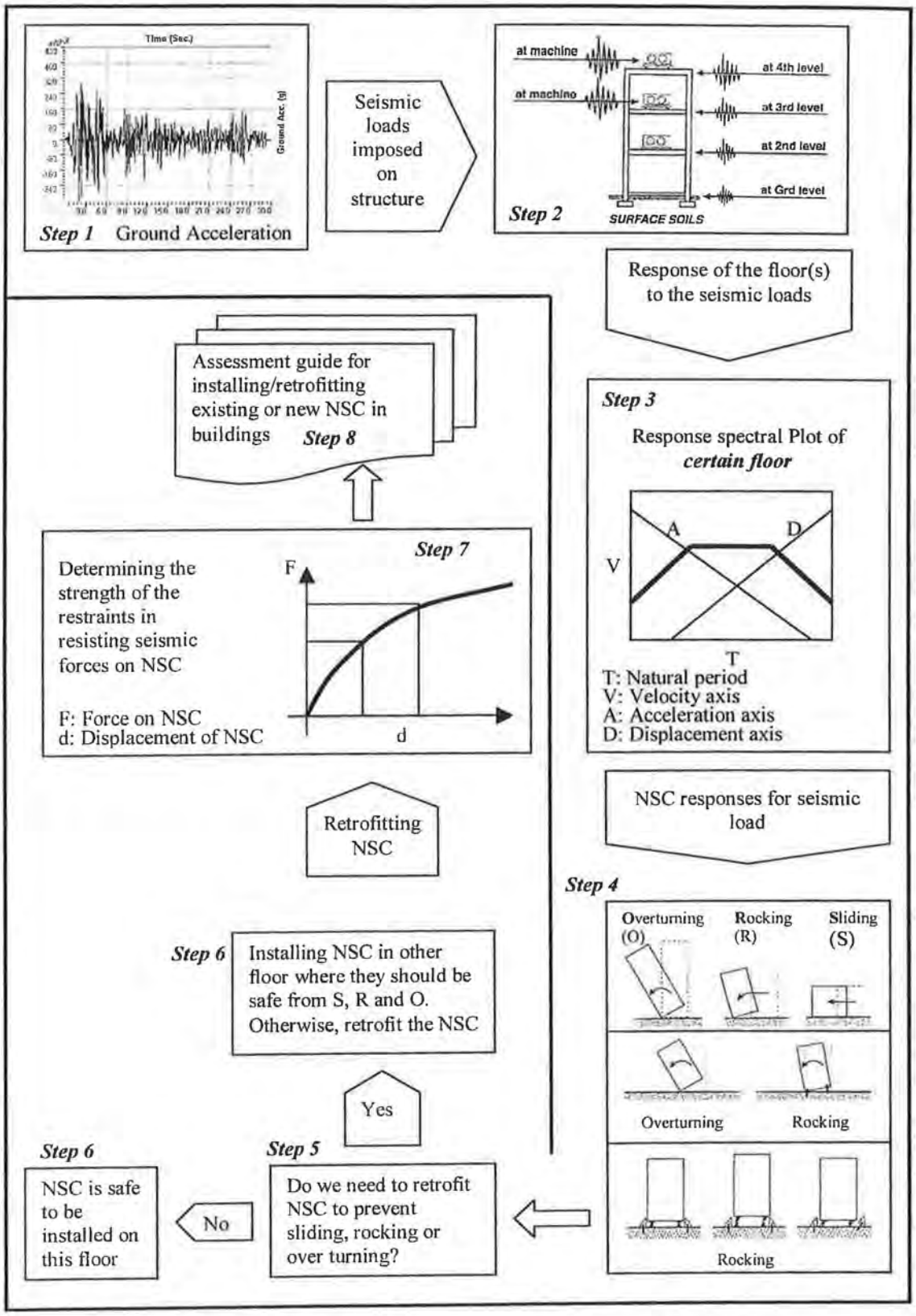

Figure 3. Schematic representation of the NSC assessment procedure

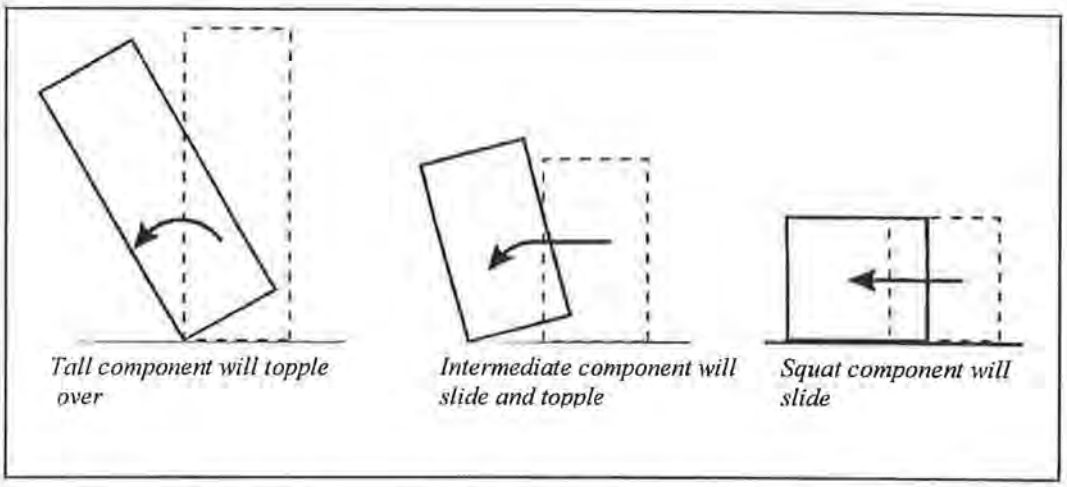

Figure 4. Effect of component height on the components response to seismic loads

The damage mechanisms of floor mounted and freestanding components could be linked to the Ao-Vo-Do (object peak acceleration – object peak velocity – object peak displacement) parameters (see Figure 5a) for determining the component vulnerability. The component is deemed safe from overturning if either Do is insufficient to move its centre of gravity (c.g.) far enough to its edge or if Ao is insufficient to result in static instability (see Figure 5b). Vo represents the strain energy stored in the NSC when responding to seismic actions. Rocking of the component might cause damage to the restraints or the attached accessories (such as pipes). The Ao-Vo-Do parameters can also be combined to obtain refined estimates in situations where initial assessment shows non-compliance.

Should the initial DB (Displacement Base) assessment based on Do shows non-compliance, drift may be re-calculated based on Vo using energy principles. Should the first two assessments show non-compliance, drift may be re-calculated again based on Ao using conventional principles of force and stiffness. Interestingly, the component is deemed satisfactory should any one of the three assessments show compliance.

This is justified by the fact that each of the Ao-Vo-Do lines making up the tri-linear envelope represents an upper bound estimate of the seismic demand as shown in Figure 5a. This new modelling framework is in significant contrast with the contemporary acceleration based approach, which often requires the natural period of both the component and the building to be determined, or else the "Ao envelope" would be overly conservative. Flexibility and versatility is clearly lacking in the traditional force-based approach. Refer Lam and Gad (2002) for further details.

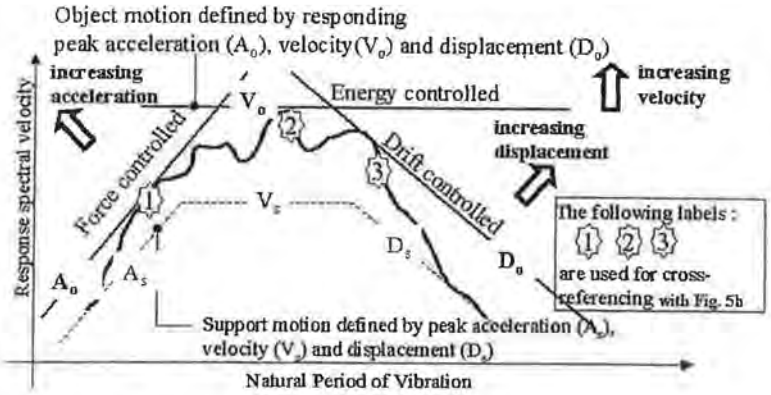

Fig. 5a Proposed generalized floor spectrum mode

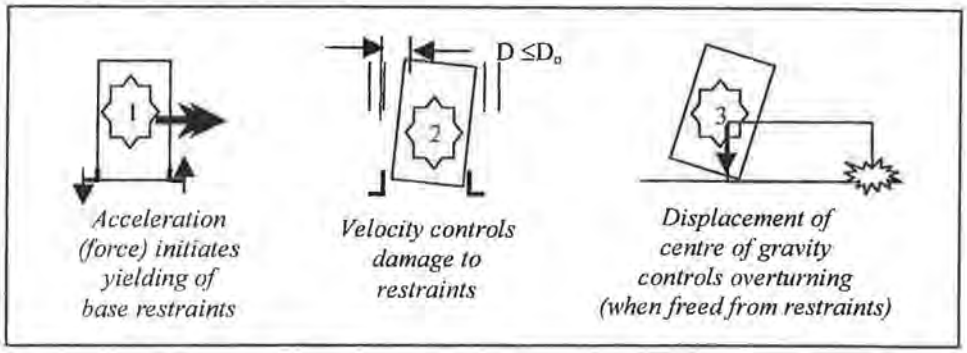

Fig. 5b Floor mounted component response

Proposed Experimental Program

An experimental program using the shaker table has been planned for the research. A physical model will be built with adjustable weights and drawers in order that NSC of varying dimensions and centre of gravity properties could be tested repetitively on the shaker table without requiring a large number of specimens to be made. The testings will cover both restrained and unrestrained components with different motion sensitivity behaviour. Real components will also be tested for comparison with testing of the model specimen. Different floor surface finishes will be used in the testing to simulate a whole range of conditions that are likely to be encountered in practice. Importantly, equipment will be tested in accordance with different performance objectives.

Conclusions

Field surveys conducted in Melbourne show a general lack of restraints on components compared with overseas recommendations. Retrofitting every NSC in all building facilities is clearly prohibitively costly and hence not feasible to implement. The research is targeted at modelling vulnerability accurately in order that limited resources could be directed effectively to avert potential high-consequence failures. The structuring of the research into four distinct phases in developing a practical and reliable

assessment procedure has been outlined. An innovative feature in this development includes the broadband modelling of the floor motion and the associated scanning procedure which models the likelihood of overturning.

Acknowledgments

The authors would like to acknowledge managers of properties/facilities who provided us with great assistance in our field surveys. The investigation has benefited a great deal from the very useful information provided by the Canadian company *Terra Firm Earthquake Preparedness Inc.* on their website. The permission given by this company to publish some of their photos is also gratefully acknowledged.

References

Arnold C, Hopkins D and Elesser E (1987), "Design and detailing of architectural elements for seismic damage control", Building Systems Development Inc., KRTA Ltd. And Forell/Elesser Engineering Inc

Chopra A. K (2001), "Dynamics of Structures theory and application to earthquake Engineering", Prentice-Hall, Inc. United State of America.

Brunsdon, D and Clark, W. (2001), "Modern multi-storey buildings and moderate earthquakes", Proceedings of the Annual Technical Conference of the New Zealand Society for Earthquake Engineering, Paper no.3.02.01.

Hall JF(1995), Technical Editor, "Nonstructural Damage, Northridge Earthquake of January17, 1994 Reconnaissance Report", Earthquake Spectra, Vol.1 Publication 95-03, 453-513.

Henry J.L. (1990), "Earthquakes An Architect's Guide to Nonstructural Seismic Hazards", John Wiley and Sons, Inc. United States of America.

Lam, N. and Gad E. (2002) "An Innovative Approach to the Seismic Assessment of Non-Structural Components in Building", Proceeding of a conference held by the Australian Earthquake Engineering Society, Paper No.10.

Monto G., Nuti C. and Santini S. (1996). "Seismic assessment of hospital systems", Proceedings of the 11th WCEE, Acapulco, Mexico.

Naeim F (1999), "Lessons learned from performance of non-structural components during the January 17, 1994 Northridge Earthquake – case studies of six instrumented multistory buildings", Journal of Seismology and Earthquake Engineering, 2(1), 47-57.

Naeim F (2001), "The Seismic Design Handbook CD-ROM", John A. Martin and Associates, Inc. Los Angeles, United States of America.

Phan LT and Taylor AW (1996), "State of the art report on seismic design requirements for nonstructural building components", US National Institute of Standards and Technology Interim Report (NISTR) 5857.

STEEL PLATED SEISMIC RETROFIT FOR RC COLUMNS IN SOFT-STOREY FRAMES

M. GRIFFITH, Y. WU AND D. OEHLERS
THE UNIVERSITY OF ADELAIDE

AUTHORS:

Mike Griffith and Deric Oehlers have been at The University of Adelaide since 1988 where they now both hold the title of Associate Professor. Dr. Griffith's main research focus is on earthquake engineering for concrete and masonry construction while Dr Oehlers' research interests mainly focuses on composite structures. Dr Wu obtained his PhD at The University of Adelaide in 2002 and has recently commenced working as a post-doctoral research fellow at the same university. The result of Dr Wu's PhD research is the subject of this paper.

ABSTRACT:

The main focus of this paper is to describe an innovative new retrofit technique that consists of attaching steel or FRP plates to the flexural faces of a concrete column using bolts. This technique is suitable primarily for columns having rectangular cross-sections (where conventional jacketing does not produce sufficient confinement) and in situations where lateral loading induces predominately a single plane of bending (as opposed to biaxial bending). Furthermore, it is assumed that the column in its unretrofit state suffers primarily from a lack of displacement capacity, or ductility. Experiments have confirmed the ability of this retrofit approach to enable columns to sustain their gravity loads at drifts well in excess of 2.5% drift. Numerical models that have been validated against the experiments indicate that an optimized retrofit solution can increase the drift capacity to nearly 10%.

INTRODUCTION

One of the major problems with regard to the seismic behaviour of reinforced concrete (RC) columns is flexural failure due to a lack of compressive strength and/or ductility of the concrete within the plastic hinge zone, namely plastic hinge failure (Seible et al. 1997). Until the early 1990s, the most common method for retrofitting RC columns was by jacketing, such as by installing grout-injected steel jackets (Chai et al 1991) or by simply increasing the RC cross-section with additional reinforced concrete (Rodriguez and Park 1994). More recently, the use of external fibre reinforced polymer (FRP) wrapping has become widespread. However, the confinement effect of steel/FRP wrapping is much less effective for square or rectangular columns than for circular columns (Mirmiran et al 1998). Efforts have been made to improve the confinement ability of rectangular jackets by increasing their out-of-plane flexural stiffness, such as by using additional stiffeners (Chai et al. 1990). However, the improvement was not satisfactory. Another solution was to enclose the square/rectangular columns by circular/elliptical jackets, which was found to be very effective (Priestley and Seible 1995). However, this technique is not always suitable when significant changes to the size or shape of the column are not desirable.

In a new effort to tackle this problem, an alternative procedure of partial interaction plating illustrated in Fig.1 has been investigated. The top of the stub column in Fig.1(a) is equivalent to the point of contraflexure of a column in a sway frame. Steel plates are bolted to the opposite faces of the rectangular column as shown in Figs.1(a) and 1(d). When the lateral force F is directed to the left as shown in Fig.1(a), the restraint at the bottom of the left-hand plate acts as "fixed" as in Fig.1(b). In contrast, the right-hand plate can rise as shown in Fig.1(c) because the restraint on the right is comparatively small as indicated in Fig.1(b). Reversal of the force F, such as occurs under seismic loading, simply reverses the restraint conditions. Hence, the essence of this technique is that the longitudinal strength of the plate directly increases the capacity of the compression face without significantly increasing the capacity of the tension face. In this way, the compressive resistance of the RC cross-section is increased and the crushing of concrete is delayed, which in turn improves the sectional flexural strength and/or ductility. This new approach of composite plating is, therefore, completely different from traditional jacketing which relies on lateral confinement to improve the material properties of the concrete.

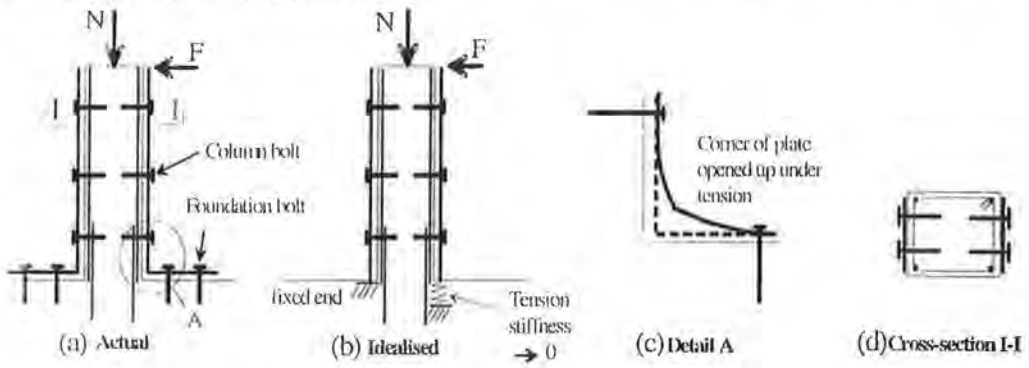

Fig.1 Composite plated column

Theoretical studies (Wu, Griffith and Oehlers 2001) have shown that this technique can be used to improve either the strength or ductility, or both, of RC columns that have potential compression failure problems in the plastic hinge region. Detailed theoretical studies on the various effects of the plating system have been published elsewhere (Wu, Oehlers and Griffith 2002) and a design procedure has been developed. In this paper, tests on composite plated columns are reported which confirms the theoretical predictions. Full details of these tests are given in Wu (2002).

TEST COLUMNS AND MATERIAL PROPERTIES

A typical column specimen (200 x 200mm with 4Y16 bars and R10 stirrups at 100mm) is shown in Fig.2 where it can be seen that the columns were tested horizontally. The pin support in Fig.2(a) is the top of the cantilever column and the stub-end represents the base of the cantilever column (or a beam-column joint). There are actually two cantilever columns in each test specimen shown in Fig.2(a) which were used for two different tests by temporarily strengthening one side while testing the other side.

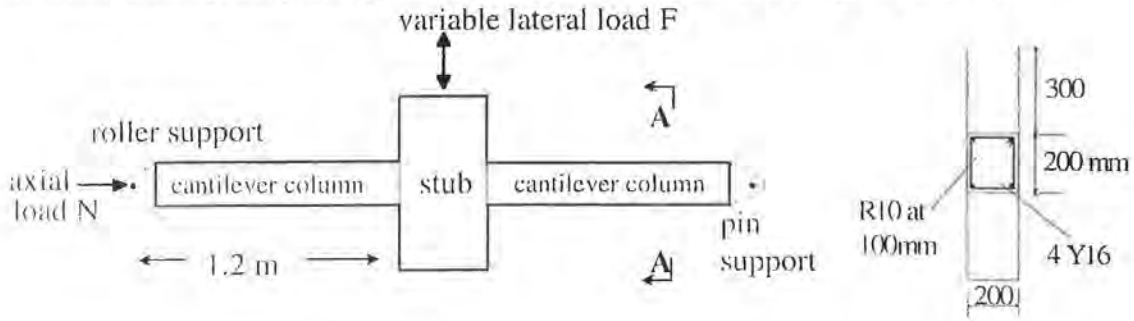

(a) Elevation (b) Section A-A

Fig.2 Test scheme

During each test, side plates were attached after which a constant axial load of 360kN, (22.5% of the column squash load N_c) was applied to the specimen under load control. Then, the vertical load jack was used to impose lateral displacements to the column. Three columns were subjected to monotonically increasing static load and two columns were subjected to quasi-static cyclic loading. All tests were terminated once a column could no longer sustain its axial load. The main test variables were the load type (monotonic static versus quasi-static cyclic) and the stiffness of the plating system. The stiffness of the plating system depends on the stiffness of the steel plate and the stiffness and number of the column bolts. The influence of plate stiffness was studied by using two different plate thicknesses. The same type of bolt was used in all tests. However, the bolting stiffness was varied between full-interaction plating and partial-interaction plating. Full-interaction plating consisted of both gluing and bolting the plate onto the face of the column, which prevented relative movement, or slip, between the plate and the column. For partial-interaction plating, the plate was connected to the column face by bolting only. The basic plating geometry is shown in Fig. 3.

Each test column was named with a specific code reflecting the key features of the test, as described below:

1. 1AMR – Monotonic loaded test of RC column without plating.

2. 2AMF12 – Monotonic loaded test of the full interaction plated column with 12mm thick mild steel plate glued and bolted on the compression face.
3. 1BMP6 – Monotonic loaded test of the partial interaction plated column with 6mm thick mild steel plate bolted on the compression face.
4. 3ACR – Cyclic loaded test of RC column without plating.
5. 4ACP6 – Cyclic loaded test of the partial interaction plated column with 6mm thick mild steel plates bolted on both the compression and tension sides.

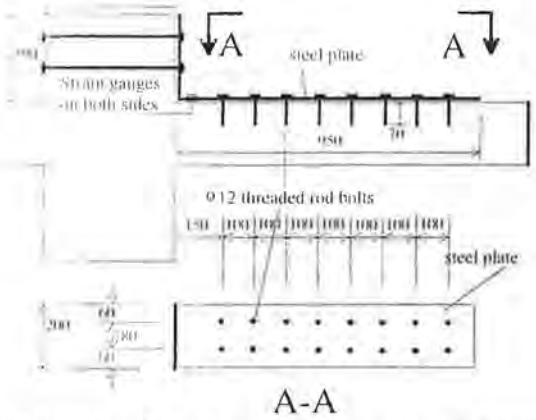

Fig.3 Details of partial interaction plating

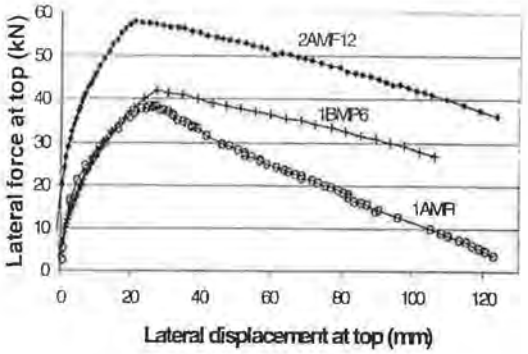

Fig.4 Monotonic test results

Material tests were conducted to obtain the properties of the concrete, reinforcing bars, steel plates, and anchor bolts, and the results are summarised in Table 1. The properties of the partial-interaction connection are not only related to the properties of the bolt, but also related to the properties of the concrete and the steel plate. Bolt shear tests were conducted from which the values for yield strength and elastic stiffness per bolt of 30kN and 23kN/mm, respectively were obtained.

Table 1 Material properties

Material	Strength (MPa)	Young's Modulus ($x10^3$ MPa)
concrete	$f_c' = 40$	27.9
Y16 reinf. bar	$f_{sy} = 548$	197
R6 reinf. bar	$f_{sy} = 690$	-
12mm steel plate	$f_{sy} = 307$	199
6mm steel plate	$f_{sy} = 307$	200
ϕ12 bolts	$f_{sy} = 750$	-

COLUMN TEST RESULTS

Monotonic tests

The response curves for the three monotonic tests are given in Fig.4 where it can be seen that the strength and ascending branch stiffness of the 6mm thick partial interaction plated column (1BMP6) and the un-plated benchmark column (1AMR) are similar. The

main difference in response between these two columns is that the plated column had a less rapid loss of strength beyond the peak displacement. The 12mm thick full interaction plated column (2AMF12), in contrast, was much stiffer and approximately 50% stronger than the reference column and it had a similar softening response to specimen 1BMP6. Interestingly, the maximum strength for all three monotonically loaded columns was reached at roughly the same displacement. Failure was deemed to occur once a test specimen could no longer maintain the constant axial load of 360kN. For specimens 1AMR and 1BMP6, this occurred at displacements of 122.4 mm and 105.6mm, respectively. Specimen 2AMF12 was still able to maintain the constant axial load at a lateral displacement of 123.4mm (≈10% drift) but the test was stopped at this point since the maximum travel distance of the test rig had been reached.

The extent of final damage to the three specimens is depicted in Fig.5. The benchmark column 1AMR failed due to excessive concrete crushing. The partial interaction plated column 1BMP6 failed due to buckling of the steel plate (refer Fig.5(b)). Significant concrete crushing in the plastic hinge of the column occurred after buckling of the plate. The full-interaction plated specimen 2AMF12 was tested to the maximum travel distance of the test rig. No excessive sign of distress in terms of instability was observed in the test, except one major tension crack located about 100mm away from the face of the stub. The bond between the steel plate and the RC column was still intact and no concrete crushing was observed in the compression zone (refer Fig.5(c)). It is also worth noting that a small amount of concrete crushing was noticed where the plate bears onto the RC joint for the 6mm plated column, as shown in Fig.5(b). This zone did not occur in the 12mm plated column (Fig.5(c)).

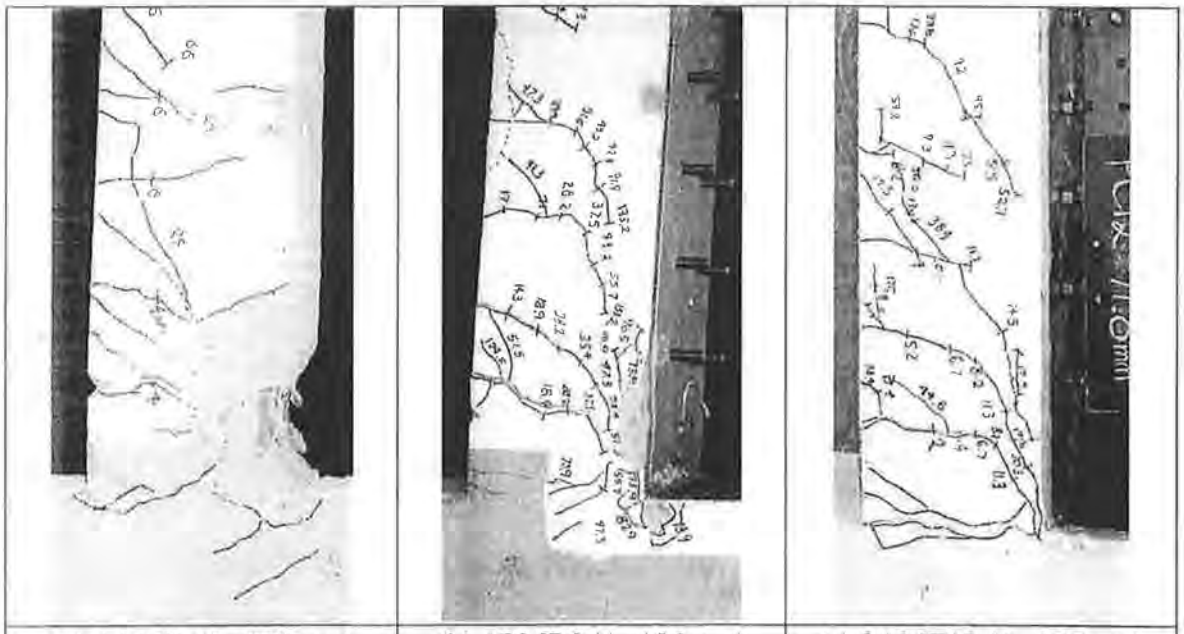

(a) 1AMR (Δ=120mm) | (b) 1BMP6 (Δ=106mm) | (c) 2AMF12 (Δ=125mm)

Fig.5 Conditions of monotonically tested specimens

Cyclic test results

The results from the cyclic tests are shown in Fig.6 for specimens 3ACR (unplated) and 4ACP6 (with 6mm plate). For comparison, the response curves are superimposed with

the envelope curves highlighted by thick lines. From these plots, it can be seen that the unplated column reached its positive maximum strength of 35kN at a displacement of 25mm (≈2% drift). At a displacement of 45mm (≈4% drift) its resistance had decreased to 80% of its maximum strength and it failed (could no longer sustain the axial load) due to concrete crushing at a load of -18kN and a displacement of -56mm. The condition of this column at the end of the test is shown in Fig.7(a). The 6mm partial-interaction plated column (4ACP6) reached its maximum strength of 50kN at a displacement of 25mm and its strength had reduced to 80% of the maximum at a displacement of 80mm (≈7% drift). In the test of specimen 4ACP6, early signs of concrete crushing in the plastic hinge region were noted at a displacement of about ±40mm. This crushing continued to develop until the end of the test. After the maximum upward travel displacement of -82mm was reached, the specimen was pushed down monotonically to the maximum travel of the hydraulic actuator of about +150mm displacement. The test was then stopped. The final conditions of the tested specimen (after removing loose concrete) is shown in Fig.7(b). Significant concrete crushing and buckling of the steel plate was evident at this maximum position, as shown in Fig.7(c). However, as the buckling was towards the concrete side, instability did not occur so that the specimen continued to hold the axial load.

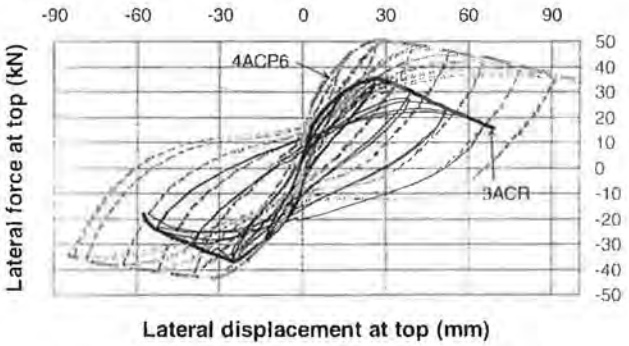

Fig.6 Comparison of cyclic test results

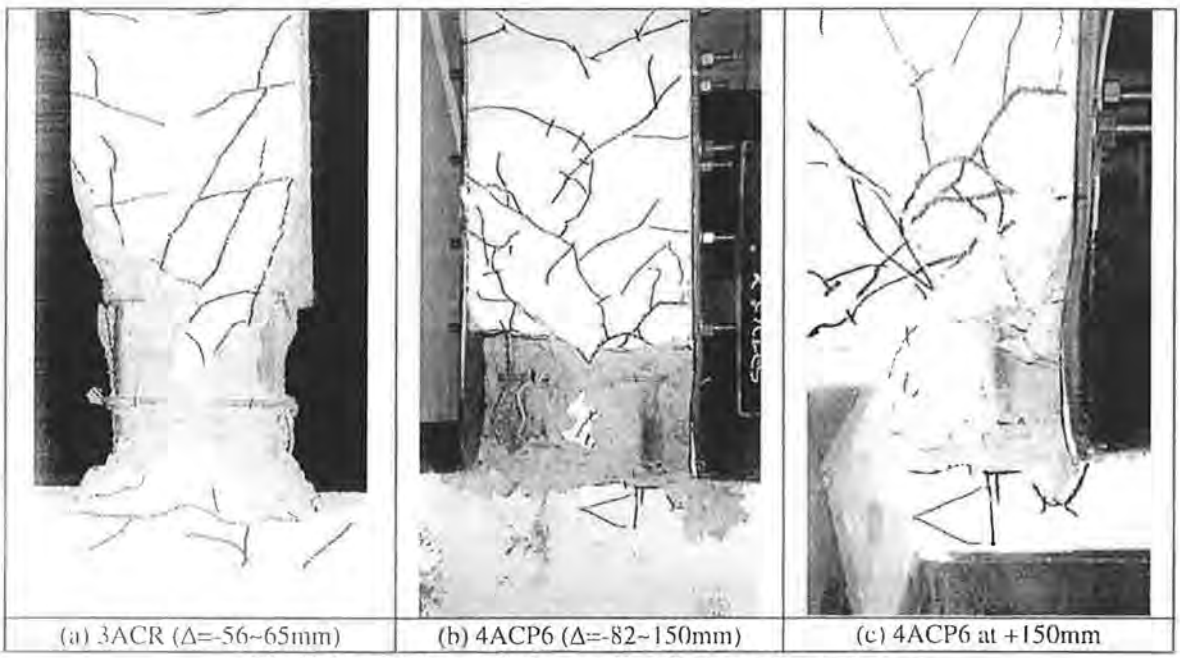

(a) 3ACR (Δ=-56~65mm)	(b) 4ACP6 (Δ=-82~150mm)	(c) 4ACP6 at +150mm

Fig.7 Conditions of the cyclically tested specimens

DISCUSSION OF TEST RESULTS

In order to quantify the extent to which this new retrofit technique is able to improve the load-deflection behaviour of the benchmark column, the displacement ductility factor, μ_Δ, was calculated for each column. The displacement ductility factor is defined here as the ratio of the displacement when the post-peak lateral resistance has decreased by 20% (to 80% of the peak load) divided by the yield displacement. The yield displacement for the columns is the displacement at the peak point of the response curve where the tension bars first yield. For the three columns in the monotonic tests, the displacement ductility factor was found to be 1.6 for the reference column (1AMR), 2.7 for column 1BMP6 and 3.8 for column 2AMF12. Clearly, the steel plating has improved the member ductility and, in the case of column 2AMF12 also the strength and stiffness. The corresponding ductility factors for the two cyclically loaded columns were 1.8 for the un-plated column (3ACR) and 3.2 for the 6mm partial composite plated column (4ACP6). These results are generally consistent with the results from the monotonic tests and suggest that the new retrofit scheme can also be used for seismic applications. While the displacement ductility values observed in the tests were modest, numerical studies indicate that a displacement ductility of 7 would be obtained for a 200mm square column with a 12mm thick bolted plate (not glued as for the test specimen) (Wu, 2002).

The difference in the results for the static and cyclic loaded 6mm and 12mm plated columns (1BMP6 and 2AMF12 versus 4ACP6 and 3ACR) was due to the fact that the specimen 1BMP6 was a "B" specimen whereas the other 3 specimens were all "A" specimens. "B" specimens were the 2nd columns tested on a double-cantilever specimen. In spite of the protection given to the non-tested end in the "A" specimen tests, yield penetration into the beam-column stub affected the stiffness and to a lesser degree the strength of the subsequent "B" test specimens. Nevertheless, the results from both the static and cyclic tests indicate that this retrofit technique can be used to address both strength and ductility deficiencies. The results of numerical modelling (Wu et al, 2002) also show that it is possible to improve ductility without increasing a column's strength. This attribute is potentially very attractive where strength increases are not desirable due to the limited strength of adjacent members or foundations.

It should be noted that the ability of these columns (even the unplated specimens) to withstand such large drifts while supporting a large axial load (22% of ultimate) is well beyond normal expectations. For the unplated columns, this was due entirely to the confinement afforded by the R10 bars located at 100mm spacing (D/2) within the hinge zones. Finally, the cyclic tests demonstrated that no substantial cyclic degradation was observed in the plated columns. This characteristic is extremely desirable for seismic applications where structural members must be able to withstand repeated cycles of loading without suffering significant reductions in strength and stiffness.

SUMMARY AND CONCLUDING REMARKS

This experimental work has demonstrated that plating columns, which utilise composite partial interaction, is effective for retrofitting RC columns with a potential plastic hinge failure mode. The composite plating system has been shown to effectively:

- increase both the strength and ductility of RC columns; or
- increase ductility without significant increase in strength.

In composite plating, the longitudinal strength of the steel plate is used to prevent concrete crushing. This technique is effective because the special joint detail allows the plate on the tension face of the column to "open up" without attracting significant tension force while the plate on the compression face of the column is able to attract substantial compression force, thereby reducing the compression strain (and stress) in the compression zone of the concrete cross-section and delaying the onset of crushing.

This technique, in its current form, would be applicable primarily for columns subject to one-way bending. Further research is underway to investigate the plating scheme that can take load from any direction or under two way bending.

REFERENCES

Chai, Y.H., Priestley, M.J.N., and Seible, F. (1991). "Seismic retrofit of circular bridge columns for enhanced flexural performance." *ACI Structural Journal*, **88**(5), 572-584.

Chai, Y.H., Priestley, M.J.N., and Seible, F. (1990). "Retrofit of bridge columns for enhanced seismic performance". *Proceedings of the First U.S.-Japan Workshop* on Seismic Retrofit of Bridge, Public Works Research Institute, Tsukuba, Japan.

Mirmiran, A., Shahawy, M., Samaan, M., El Echary, H., Mastrapa, J.C., and Pico, O. (1998). "Effect of column parameters on FRP-confined concrete." *Journal of Composites for Construction*, **2**(4), 175-185.

Priestley, M.J.N., and Seible, F. (1995). "Design of seismic retrofit measures for concrete and masonry structures." *Construction and Building Materials*, **9**(6), 365-377.

Rodriguez, M.; and Park, R. (1994). "Seismic load tests on reinforced concrete columns strengthened by jacketing." *ACI Structural Journal*, **91**(2), 150-159.

Seible, F., Priestley, M.J.N., Hegemier, G.A., and Innamorato, D. (1997). "Seismic retrofit of RC columns with continuous carbon fiber jackets." *Journal of Composites for Construction*, **1**(2), 52-62.

Wu, Y.F. (2002) *Seismic Retrofitting of Rectangular RC Columns with Partial Interaction Plating*. PhD thesis, Dept. of Civil & Environmental Engineering, The University of Adelaide, Australia.

Wu, Y.F., Griffith, M.C., and Oehlers, D.J. (2001). *Behaviour of plated RC columns*. Dept. of Civil & Environmental Engineering, The University of Adelaide, Research report No. R173.

Wu, Y.F., Oehlers, D.J., and Griffith, M.C. (2002). "Partial interaction analysis of composite beam/column members". *Mechanics of Structures and Machines*, **30**(3), 309-332.

COMPARATIVE STUDY OF AVERAGE RESPONSE SPECTRA FROM AUSTRALIAN AND NEW ZEALAND EARTHQUAKES

TREVOR ALLEN[1], GARY GIBSON[2,1] AND JAMES CULL[1]
MONASH UNIVERSITY[1] AND ES&S SEISMOLOGY RESEARCH CENTRE[2]

AUTHORS:

Trevor Allen is a PhD candidate within the School of Geosciences, Monash University, Melbourne. He is currently investigating seismic attenuation in southeastern Australia and its implications on hazard associated with local and regional earthquakes.

Gary Gibson established the Seismology Research Centre in 1976, and has worked there since. He has worked at Phillip Institute of Technology and RMIT University since 1968, and is now an Honorary Research Associate at Monash University. His interests lie in observational seismology and its practical applications.

James Cull is the Head of the School of Geosciences, Monash University. His interests include the development and application of geophysics involving electrical and EM methods, rheology, crustal heat flow, and mineral exploration.

ABSTRACT:

Average 5% damped pseudo-velocity response spectra have been calculated from the strong motion records of several moderate-magnitude, shallow crustal earthquakes from southeastern Australia and New Zealand. Results indicate that the spectral shape for the Australian events are typically dominated by higher levels of short-period ground motion relative the spectral shape from New Zealand earthquakes of similar magnitude. Consequently we observe shorter-duration ground motion for Australian events, coupled with high stress drops and a more compact source. In contrast, source parameters calculated from the spectra of New Zealand earthquakes typically indicate lower corner frequencies and consequently, lower stress drops.

These data identify significant characteristics of strong ground motion in Australia and will provide the framework for the development of attenuation models based on recorded ground motion. Further research in this field will have implications for future revisions of the proposed Joint Australia/New Zealand Loading Standard, AS/NZS 1170.4.

1. INTRODUCTION

The development of the Joint Australia/New Zealand Loading Standard, AS/NZS 1170.4, presents the need for an increased awareness of source characteristics for Australian and New Zealand earthquakes, in particular, the effect that strong ground motions have on large civil constructions. Given the differences of the seismotectonic regimes between the intraplate and interplate regions of Australian and New Zealand, respectively, the nature of strong ground motion from an earthquake source and the associated hazard must be considered independently for each region.

Studies of earthquake hazard in Australia have been limited by a relatively short recording period and sparse seismograph network, especially prior to 1960. Because of Australia's wide distribution of epicentres and limited strong motion records, the evaluation of empirical response spectral attenuation relationships has been difficult.

The first earthquake intensity attenuation relationships developed entirely from Australian earthquake data were those compiled by Gaull *et al.* (1990). Prior to this work, hazard maps were largely compiled using models derived from international studies. Gaull *et al.*'s relationships used conversions of Modified Mercalli Intensity to peak ground acceleration (in m/s^2) or velocity (in mm/s) employing the empirical relations of Newmark and Rosenblueth (1971). The subsequent hazard maps, combined with modifications from an earthquake engineering draft committee, culminated in the development of the 1991 Earthquake Hazard Map of Australia (Standards Australia, 1993). Over the past decade, normal practice in Australia has been to use spectral attenuation functions derived in areas with similar geological and tectonic characteristics. Eastern Australia is characterised by levels of attenuation a little higher than world average, while central and western Australia is typified by relatively low attenuation. Most Australian earthquakes appear to have relatively high stress drops. This makes eastern Australia somewhat comparable with western North America (but with higher stress drop), while central and Western Australia are comparable with central and eastern North America. Recently, Lam and Wilson (2003) have provided attenuation models for Australia by combining information derived from local seismicity with generic information from international models.

Owing to the comparatively higher levels of seismicity observed in New Zealand, seismic attenuation has been modelled extensively through both the empirical evaluation of empirical response spectra (e.g. Zhao *et al.*, 1997; McVerry *et al.*, 2000) and by conversion of earthquake intensity (e.g. Dowrick and Rhoades, 1999).

Using software developed specifically for this study, spectral shapes of response spectra for southeastern Australian and New Zealand earthquakes are evaluated and compared with a view to provide recommendations for future revisions of the joint Australasian loading standard, AS/NZS 1170.4.

2. SEISMICITY OF AUSTRALIA AND NEW ZEALAND

Like most intraplate regions, Australian earthquakes tend to be shallow and are typically restricted to a seismogenic zone within the upper 20 km of the crust. Given that the

earthquakes are shallow, it is not uncommon for the larger events to be associated with surface rupture (McCue, 1990). Recent studies by Allen *et al.* (in press) indicate that Australian earthquakes typically produce higher than average stress drops within a high horizontal stress regime (Denham *et al.*, 1979). It is typically found in observation that *in situ* stress is inversely related to earthquake recurrence (i.e. high *in situ* stress typically gives a low *b* value; Urbancic *et al.*, 1992). This is consistent with Australian observations.

In contrast to the stable continental setting of Australia, New Zealand straddles the boundary between the Indo-Australian and Pacific plates. The relative plate motion in New Zealand is expressed by a complex assemblage of active faults, coupled with a moderately-high rate of seismicity and a relatively high *b* value (Stirling *et al.* 2002). The plate boundary beneath New Zealand comprises the Hikurangi (North Island) and Fiordland (far south of South Island) subduction zones which dip in the opposite sense relative to each other. Active tectonic motion is accommodated by the faults of the axial tectonic belt which traverse much of the South Island between the two subducting slabs (Stirling *et al.*, 2002). The Alpine Fault (central South Island) facilitates the release of much of the strain energy produced by the relative plate motion. Geologic evidence on the Alpine Fault indicates that the fault has produced several large-to-great earthquakes with recurrence intervals of hundreds of years, however, it has not produced such earthquakes in historic times (Stirling *et al.*, 2002). In addition, high-to-moderate rates of moderate seismicity are observed in the crust above the two subduction zones.

3. METHODOLOGY

Earthquake response spectra specify the maximum dynamic response (i.e. maximum displacement, velocity or acceleration) of a single-degree-of-freedom (SDF) system in response to an excitation force, such as that due to an earthquake or a blast. The maximum response of the system depends upon the ground motion, coupled with the natural period and intrinsic damping of the structure which characterises the structure's capacity to dissipate ground-generated energy.

Response spectra are typically prepared by calculating the dynamic response of a SDF system subjected to ground motion over a range of natural frequencies and damping values ξ. The resulting motion of the structure is $y(t)$ and the response $u(t)$ is evaluated through numerical integration of an earthquake time series using Duhamel's integral

$$u(t) = -\frac{1}{\omega_D}\int_0^t \ddot{y}(\tau)e^{-\xi\omega(t-\tau)}\sin\left[\omega_D(t-\tau)\right]d\tau \qquad (1)$$

where ω is the angular natural frequency and $\omega_D = \omega\sqrt{(1-\xi^2)}$ is the damped natural frequency. The damping ratio is usually small for structural systems (i.e. $\xi << 1$); therefore $1-\xi^2 \approx 1$ and $\omega_D \approx \omega$ (Paz, 1997). The integral in relation (1) therefore represents a convolution between the ground acceleration and the response of the oscillator impulse.

In the current study, horizontal, 5% damped response spectra are normalised from synthetic accelerograms approximated at a hypocentral distance of r = 5 km from the source. Source excitation $A_i(f)$ is firstly approximated from Fourier analysis following

$$A_{ij}(f,r) = A_i(f)\, e^{\frac{-\pi f r}{v Q_a(f,r)}} \cdot G(r) \tag{2a}$$

for the ith event, where $A_{ij}(f,r)$ is the recorded Fourier amplitudes recorded at site j and v is the S-wave velocity at the source. The anelastic attenuation parameter (or *apparent quality factor*) defined by Allen (2003) follows the power law form $Q_a(f,r) = Q_r(r) f^{\eta(r)}$, where f is frequency, $Q_r(r)$ is the apparent quality factor at f = 1 Hz and $\_(r)$ is a numerical constant at a distance r. We use a geometrical spreading coefficient $G(r)$ of r^{-1} for $r \leq 80$ km and $(r_0 r)^{-1/2}$ for $r > 80$ km, where r_0 = 80 km; the approximate distance where geometrical spreading becomes less severe owing to surface-wave arrivals (Castro *et al.*, 1997). Allen (2003) has demonstrated that a geometrical spreading coefficient given by these relations results in robust source scaling that yields earthquake source parameters that do not vary significantly with source-receiver distance.

Since it is not always practical for to identify the excitation directly at the source for engineering purposes, the second step is to simulate the decay of Fourier spectra $A_{ik}(f,r)$ to some hypothetical site k to an arbitrary distance of 5 km, approximating the closest source-receiver distance to rupture along the causative fault following

$$A_{ik}(f,r) = \frac{1}{5} A_i(f)\, e^{\frac{-5\pi f}{v Q_a(f,r)}}. \tag{2b}$$

Response spectra at 5% damping are subsequently evaluated for each of the simulated accelerograms and the geometric mean is obtained. Using the methods presented above, we handle the average response spectra similarly to Fourier spectra to approximate the spectral decay at additional sites k located regularly; r = 5 to 200 km from the source. Although this approach is not technically correct, it has been demonstrated to give reasonable approximations of the decay of response spectra without performing time consuming response spectral calculations at multiple source-receiver distances (Allen, 2003). Spectra are representative of average ground motion at a range of distances. Complications arising from complex phase arrivals at different hypocentral distances are not considered in detail.

In estimating the amplitude of earthquake spectra near the source (i.e. r < 10 km), the approximation of a point source becomes insufficient to describe an earthquake which has a characteristic rupture size. This is particularly significant for larger events, where observed ground motions depend on the minimum distance of the receiver to the rupture surface of the causative fault and the directivity of the rupture pulse (Somerville, 2003). At hypocentral distances comparable to the dimensions of fault rupture (e.g. rupture length $r_d \approx r$), published spectra typically plateau at some maximum amplitude. For larger hypocentral distances ($r >> 1$ km), the ratio $(r + r_d)/r \rightarrow 1$ and spectral

amplitudes tend to decay from according to geometrical spreading and anelastic attenuation. These factors must be considered when developing attenuation models for moderate-magnitude earthquakes.

4. ATTENUATION PARAMETERS

Attenuation parameters used in the present study were evaluated using alternative methodologies based on the conventional two-station spectral ratio method (Allen, 2003). To prevent the exponential term in relation (2) approaching infinity as $r \_ 0$, we limit Q_r to a minimum value of 10. $Q_a(f,r)$ for southeastern Australian earthquakes is therefore expressed by the bilinear function (Allen, 2003)

$$Q_a(f,r)_{r\le 150} = \left(1.85r + 10e^{-\frac{r}{10}}\right) f^{(0.96-0.0039r)} \quad \text{(AUS)}, \qquad (3a)$$

$$Q_a(f,r)_{r>150} = (0.42r + 212.11) f^{(0.50-0.0003r)}$$

For consistency, we evaluate similar $Q_a(f,r)$ functions using available strong ground motion records from shallow New Zealand earthquakes. These functions are quantitatively defined as

$$Q_a(f,r)_{r\le 150} = \left[8.8 + \left(0.74r + 1.2e^{-\frac{r}{10}}\right)\right] f^{0.97} \quad \text{(NZ)}. \qquad (3b)$$

$$Q_a(f,r)_{r>150} = 120 f^{0.97}$$

Relations (3a) and (3b) represent average anelastic attenuation parameters and have each been derived from multiple events in their respective regions, having a wide range of epicentral locations and magnitudes to remove bias from specific geologic terrains and source radiation patterns.

Figure 1 indicates a comparison of $Q_r(r)$ and $\_(r)$ for Australia and New Zealand. At near-to-intermediate hypocentral distances ($r < 150$ km), $Q_r(r)$ increases regularly with r for both regions. The change in slope observed at approximately 150 km (Fig. 1a) is most likely due to the dominant travel path being either in the crust or mantle, above or below the Moho. The regularity of the inflection near 150 km suggests a similar crustal thickness exists for southeastern Australia and New Zealand. Beyond 150 km, $Q_r(r)$ for Australia continues to increase regularly at a lower rate; however, $Q_r(r)$ remains consistently low for New Zealand, indicative of higher anelastic attenuation in New Zealand's upper mantle. This is most likely a response from neotectonic processes and a high heat flow regime owing to extensive volcanism, particularly in the North Island. Values of $\_(r)$ for southeastern Australia seem to be inversely proportional to $Q_r(r)$, whereas they are relatively consistent with r in New Zealand (Fig. 1b). This may be an artefact which indicates that high-frequency ground motion in New Zealand is being attenuated rapidly through continental lithosphere and therefore being masked by higher mode ambient noise levels.

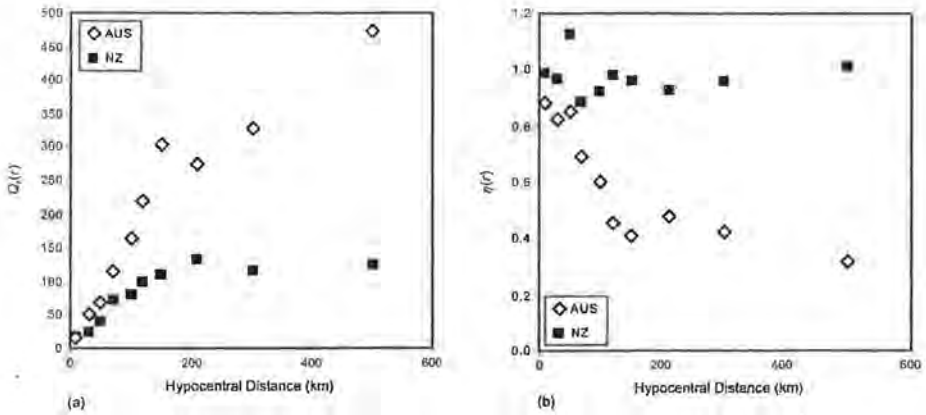

Figure 1. Anelastic attenuation parameters (a) $Q_r(r)$ and (b) _(r) evaluated for southeastern Australia and New Zealand. Note that $Q_r(r)$ increases with source-receiver distance and is typically higher in southeastern Australia (i.e. lower anelastic attenuation). _(r) is inversely proportional with $Q_r(r)$ for southeastern Australia, whereas it is relatively consistent with r in New Zealand. (After Allen, 2003).

5. DATA

Unprocessed digital short-period seismograms were obtained for selected moderate-magnitude earthquakes from the ES&S Seismology Research Centre, Australia, and from the Institute of Geological and Nuclear Sciences' GeoNet Data Centre, New Zealand. Seismogram data were subsequently corrected for instrument response and converted to accelerograms in the Fourier domain. Data presented in the current study represents a subset of the total data studied (Table 1). To enable an unbiased appraisal of response spectra from each region, the chosen events were all shallow crustal earthquakes (focal depths ranging from 11 to 18 km) of horizontal-component moment magnitude M_W 3.9 to 4.4. Seismic moment for each event was determined employing the local anelastic attenuation parameters described in relation (3) and subsequently converted to M_W following the empirical relation of Hanks and Kanamori (1979) (where M_W derived from vertical-component records follows the relationship $M_W = 0.75\,M_L + 0.34$; Allen, 2003). Brune (1970) stress drops for New Zealand earthquakes were observed to be significantly lower compared to those evaluated for southeastern Australian events of similar seismic moment (Allen *et al.*, in press).

Table 1. Events used in average response spectra calculations. The character 'M' represents events which have epicentres in Mesozoic terranes, whereas, 'P' represents events of origin in Palaeozoic terranes.

Place, Country	Date	Longitude (°E)	Latitude (°N)	Depth (km)	M_W	Terrane Type
Thomson Reservoir, AUS	1996-09-25	146.422	-37.863	11	4.3	P
Corryong, AUS	1998-07-17	148.005	-36.441	12	3.9	P
Boolarra South, AUS	2000-08-29	146.245	-38.402	15	3.9	M
Mt Pye, NZ	2000-10-12	169.236	-46.428	15	4.0	M
Charles Sound, NZ	2000-11-14	167.038	-45.096	18	4.4	M

6. RESULTS AND DISCUSSIONS

Averaged response spectra calculated for both Australian and New Zealand earthquakes of similar magnitude indicate very different spectral shapes. Empirically predicted ground motions are generally consistent with the published attenuation function of Sadigh *et al.* (1997) at hypocentral distances 50 km and greater, however, they tend to

be significantly lower near the source (Fig. 2). This may be an artefact of published functions which are principally developed for larger earthquakes such that the ratio $(r+r_d)/r$ becomes increasingly critical. Although they don't compare well with the published functions, the models presented here are consistent with response spectra calculated from individual sites at distances where we possess good quality data. This is due to different methodologies in estimating motion near the source. If this normalisation to source method proves valid, it may imply lower near-source earthquake motion which converges with published functions at very near-distances (i.e. $r < 1$ km) in southeastern Australia than is currently computed. Complications arising from complex phase arrivals were not observed to pose any significant problems; synthesised spectra at 5 km, were in general, quite consistent.

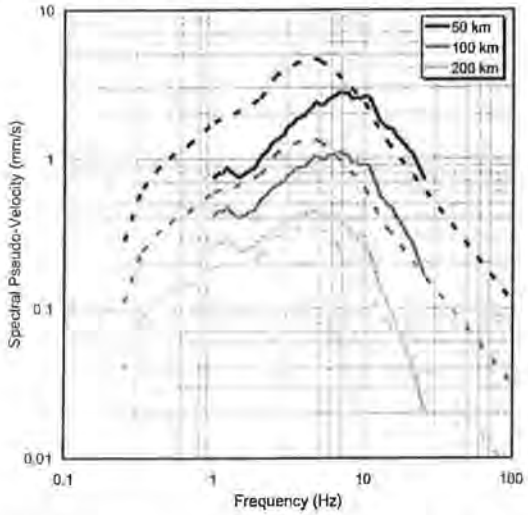

Figure 2. The decay of response spectra with hypocentral distance for the 2000-08-29 Boolarra South, M_W 3.9 earthquake. Spectral pseudo-velocity shapes are compared to the Sadigh et al. (1997) attenuation function (dashed lines) at 50, 100 and 200 km. Although not technically correct, these data define a robust approximation for the decay of response spectra with distance and are observed to be consistent with empirical site spectra.

Plotting average response spectra for events of similar magnitude, we observe that Australian earthquakes typically have greater high-frequency content (Fig. 3), and do not drop towards PGA values as quickly as in New Zealand. Normalising each of the average spectra to their peak spectral pseudo-velocity further demonstrates this observation (Fig. 4). Comparisons of response spectra evaluated for moderate magnitude earthquakes in southeastern Australia indicates that events occurring in Palaeozoic terranes (e.g. Corryong) tend to possess a greater composition of short-period motion than earthquakes that occur in or beneath younger Mesozoic terranes (e.g. Boolarra South; Fig. 4). Given that moment magnitude is derived from low-frequency spectral amplitudes, we expect near-source spectral amplitudes to be equivalent for long-period ground motions.

7. CONCLUSIONS

Using available data, new anelastic attenuation parameters $Q_a(f,r)$ have been evaluated for New Zealand to complement the existing relations for southeastern Australia (Allen, 2003). The apparent quality factor $Q_r(r)$ is observed to increase systematically with r for both regions. The change in slope observed at approximately 150 km is most likely due to an attenuation differential at the crust and mantle boundary. Overall, it was observed that the loss of elastic seismic energy through the New Zealand crust is higher than in southeastern Australia, while losses in the upper mantle is significantly higher.

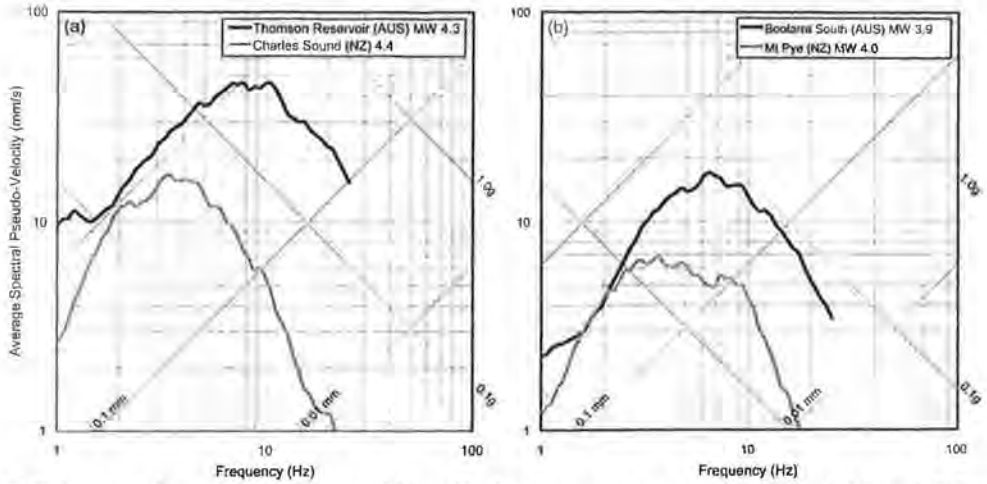

Figure 3. Tripartite plots of Australian and New Zealand average response spectra. (a) The left-hand plot indicates averaged spectral shapes at hypocentral distances of 5 km and 20 km for the M_W 4.3 1996-09-25 Thomson Reservoir (AUS) and the M_W 4.4 2000-11-14 Charles Sound (NZ) earthquakes. (b) The right-hand plot indicates average response spectra estimated at $r = 5$ km for the M_W 3.9 2000-08-29 Boolarra South (AUS) and M_W 4.0 2000-10-12 Mt Pye (NZ) earthquakes.

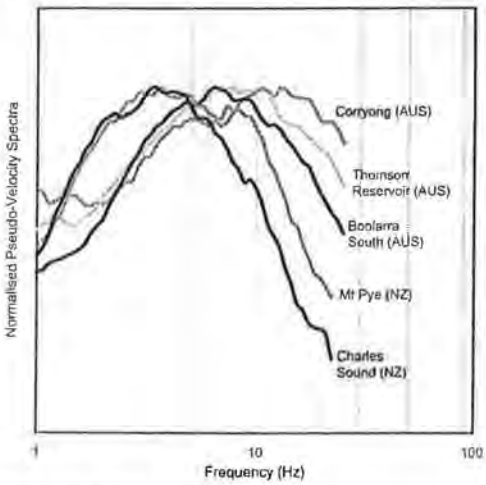

Figure 4. Synthesised 5% damped response spectra approximated at 5 km. Spectra are normalised to peak spectral pseudo-velocity. These data further indicate that Australian earthquakes yield higher components of short-period ground motion relative to New Zealand earthquakes. Furthermore, the spectral characteristics of southeastern Australian events having epicentres in Palaeozoic terrains (e.g. Thomson Reservoir and Corryong) yield additional high-frequency ground motion relative to earthquakes that occur beneath Mesozoic terrains (e.g. Boolarra South).

The chief purpose of the present study was to compare response spectra for Australian and New Zealand shallow crustal earthquakes of similar magnitude M_W. In general, it is observed that averaged 5% damped, horizontal-component response spectra produce higher levels of short-period ground motions from Australian earthquakes than observed in spectral representations of ground motion in New Zealand. Furthermore, a comparison of response spectra evaluated for moderate magnitude earthquakes in southeastern Australia indicates that events occurring in Palaeozoic terranes yield a greater composition of high-frequency motion than earthquakes that occur in or beneath younger Mesozoic terranes. As expected, the level of low-frequency motion, which characterises an earthquake's magnitude, was observed to be consistent for all earthquakes of similar magnitude.

Average response spectra evaluated in this study have provided a basis for the comparison of earthquake ground motion and seismic attenuation in southeastern Australia and New Zealand. Further research will provide a framework for the development of Australian spectral attenuation functions and design spectra, useful for future revisions of the Joint Australia/New Zealand Loading Standard, AS/NZS 1170.4.

8. ACKNOWLEGMENTS

TA would like to thank the Australian Earthquake Engineering Society for providing the funding for travel to New Zealand to undertake the research described in this paper. Graeme McVerry, John Zhao and Mark Stirling of GNS are thanked for constructive discussions while in NZ and I thank Kevin Fenaughty of GeoNet for supplying the NZ earthquake data and seismograph calibration information. I also acknowledge the staff at the ES&S Seismology Research Centre for providing access to resources and their generous cooperation for the duration of this research.

9. REFERENCES

Allen, T.I. (2003) Spectral attenuation and earthquake source parameters from recorded ground motion: Implications for earthquake hazard and the crustal stress field of southeastern Australia. PhD Thesis, Monash University, Melbourne.

Allen, T.I., Gibson, G., Brown, A. and Cull, J.P. (in press) Depth variation of seismic source scaling relations; Implications for seismic hazard for local Australian earthquakes. Tectonophys.

Brune, J.N. (1970) Tectonic stress and the spectra of seismic shear waves from earthquakes. J. Geophys. Res., Vol 75, pp 4997-5009.

Castro, R.R., Reboller, C.J., Inzunza, L., Orozco, L., Sánchez, J., Gálvez, O., Farfán, F.J. and Méndez, I. (1997) Direct body-wave Q estimated in northern Baja California, Mexico. Phys. Earth Planet. Interiors, Vol 103, pp 33-38.

Denham, D., Alexander, L.G. and Worotnicki, G. (1979) Stresses in the Australian crust: evidence from earthquakes and in situ stress measurements, BMR Journal, Vol 4, pp 289-295

Dowrick, D.J., Gibson, G. and McCue, K. (1995) Seismic hazard in Australia and New Zealand. Bull. NZ Soc. Earthquake Eng., Vol 28, pp 279-287.

Dowrick, D.J. and Rhoades, D.A (1999) Attenuation of Modified Mercalli Intensity in New Zealand earthquakes. Bull. NZ Soc. Earthquake Eng., Vol 32, pp 55-89.

Gaull, B.A., Michael-Leiba, M.O. and Rynn, J.M.W. (1990) Probabilistic earthquake risk maps of Australia. Aust. J. Earth Sci., Vol 37, pp 169-187.

Hanks, T.C. and Kanamori, H. (1979) A moment-magnitude scale. J. Geophys. Res., Vol. 84, pp 2348-2350.

Lam, N.T.K. and Wilson, J.L. (2003) The component attenuation model for low and moderate seismic regions. Proc. 7th PCEE, Christchurch.

McCue, K. (1990) Australia's large earthquakes and recent fault scarps. J. Structural Geol., Vol 12, pp 761-766

McVerry, G.H., Zhao, J.X., Abrahamson, N.A. and Somerville, P.G. (2000) Crustal and subduction zone attenuation relations for New Zealand earthquakes. Proc. 12th WCEE, Auckland.

Newmark, N.M. and Rosenblueth, E. (1971) Fundamentals of Earthquake Engineering. Englewood Cliffs: Prentice-Hall.

Paz, M. (1997) Structural dynamics; Theory and computation. New York, Chapman & Hall.

Sadigh, K., Chang, C.-Y., Egan, J.A., Makdisi, F. and Youngs, R.R. (1997) Attenuation relationships for shallow crustal earthquakes based on California strong motion data. Seism. Res. Lett., Vol 68, pp 180-189.

Somerville, P.G. (2003) Magnitude scaling of the near fault rupture directivity pulse. Phys. Earth. Planet. Interiors, Vol 137, pp 201-212.

Standards Australia (1993) Minimum design loads on structures. Part 4: Earthquake Loads, Australian Standard 1170.4-1993, Sydney.

Stirling, M.W., McVerry, G.H. and Berryman, K.R. (2002) A new seismic hazard model for New Zealand. Bull. Seism. Soc. Am., Vol 92, pp 1878-1903.

Urbancic, T.I., Trifu, C.-I., Long, J.M. and Young, P.G. (1992) Space-time correlations of b values with stress release. Pure. Appl. Geophys., Vol 139, pp 449-462.

Zhao, J.X., Dowrick, D.J. and McVerry, G.H. (1997) Attenuation of peak ground acceleration in New Zealand earthquakes. Bull. NZ Soc. Earthquake Eng., Vol 30, pp 133-158.

ESTIMATION OF NON-STRUCTURAL DAMAGE IN RESIDENTIAL LIGHT FRAMED WALLS

J. CORVETTI, E.F. GAD, M. DEISS AND J.L. WILSON
THE UNIVERSITY OF MELBOURNE

AUTHORS:

Joe Corvetti is currently a PhD Scholar in the Department of Civil and Environmental Engineering at The University of Melbourne – j.corvetti@civenv.unimelb.edu.au

Emad Gad is Senior Research Fellow, The University of Melbourne and Senior Lecturer, Swinburne University of Technology.

M. Deiss is a Research Assistant in the Department of Civil and Environmental Engineering at The University of Melbourne.

John Wilson is Associate Professor in the Department of Civil and Environmental Engineering at The University of Melbourne.

ABSTRACT:

This paper presents the results from an ongoing extensive research program into the response of residential structures to low level vibrations from mining activities. The paper focuses on typical Australian single storey brick veneer residential construction.

In several parts of Australia open cut mining and quarrying occur relatively close to residential structures. Blasting is normally used for these activities. Which induces both ground vibrations and air blasts. While mine and quarry operators have to conform to regulatory environmental limits for both ground vibrations and air blasts, there are still some local residents concerned that ground vibrations below the regulatory limits may cause damage.

As plasterboard is used widely as interior lining in Australia, experiments on "Standard Core" plasterboard have been conducted to determine the ultimate tensile stress and strain. One of the primary aims of this study is to determine the damage threshold of typical non-structural components in structures. The outcomes of this research are also directly applicable and valuable for estimating the likely damage level to residential structures from serviceability level earthquakes.

Paper No. 11

INTRODUCTION AND OBJECTIVES

For many years plasterboard has been widely used as non-structural interior cladding (or lining) for residential structures. The most commonly used type of plasterboard in Australia is the 10mm thick 'Standard Core'. The quality of Australian plasterboard is governed by the Australian Standard, AS/NZS 2588 entitled, 'Gypsum Plasterboard'. The stated objective of this standard is ".....to provide manufacturers of gypsum plasterboard with specifications covering the manufacture and performance of such plasterboard for use in domestic, commercial and industrial applications."

Residential structures often suffer from damage to non-structural components such as plasterboard and masonry. Damage in plasterboard is always identified by cracking and therefore crack widths (and lengths) are a useful way of monitoring damage in residential structures. Racking action is a classical shear mode of action which may lead to cracking, particularly in walls with openings. Racking behaviour in walls can result from the application of dynamic lateral loads such as ground vibrations transmitted from quarry and mine blasting and can also be produced by earthquakes and wind loads.

In order to resist "racking" type loads and minimise cracking, residential structures in Australia are required to include permanent bracing fitted to the wall, floor and roof framework with appropriate connections that allow the load to be ultimately transferred to the building's foundations. In the case of wall bracing, AS1684.2 – 1999 (Residential Timber Framed Construction) states that "nominal bracing" may provide up to 50% of the total bracing requirement. It also states that the bracing capacity for "nominal sheet bracing walls" lined on one side only is 0.45 KN/m and a wall lined on both sides is 0.75 KN/m. Nominal bracing is later defined as wall framing lined with sheet materials such as plywood, plasterboard, fibre cement or hardboard or the like.

The load carrying capacity of plasterboard is reduced when penetrations such as door and window openings are included in bracing or non-bracing walls. Plasterboard cracking around penetrations in walls is often diagonal in nature (refer Figure 1 – Typical diagonal cracking in plasterboard) but the cause of cracking is not always easily identified. Siskind in his book "Vibrations from Blasting" (2000) discusses specific characteristics of vibration induced cracking based on extensive investigations carried out by the US Bureau of Mines (Siskind et al., 1980 and Stagg et al., 1984). These observations include that blast induced cracks that occur in walls will tend to propagate at an angle, be located in areas of weakness such as door and window openings and be symmetrical in nature. Siskind (2000) then compares this with non-blast related damage and highlights a recent publication where some 131 different causes of cracks were identified in residential structures. Liew et al. (eJSE, 2002) have also shown that non-structural walls may be subjected to "racking" loads due in part to the stiff diaphragm action of ceilings and loading through the cornice into the plasterboard walls.

In order to predict with any degree of certainty the likelihood, severity, location and cause of plasterboard cracking in residential structures subject to blast vibrations, the stress – strain characteristics of the material must first be understood. One of the objectives of this research project is to establish, via a rigorous testing program, the material properties of 'Standard Core' plasterboard to be applied in the prediction of

cracking in structures subject to low intensity blast vibrations and hence derive damage thresholds for various loading conditions. This paper provides preliminary tension test results on 'Standard Core' plasterboard.

Figure 1: Typical diagonal cracking in plasterboard (Moore et al., 2002)

SIGNIFICANCE OF PLASTERBOARD TENSION TESTING

The Australian Standard for Gypsum Plasterboard (AS/NZS 2588), which is based upon ASTM C473 outlines a number of tests that plasterboard manufacturers are required to carry out to ensure a certain minimum level of "in-service" performance. AS/NZS2588 provides test specifications for determining the plasterboard:

- Thickness
- Bending Strength
- Edge Hardness
- Nail Pull Resistance
- Bond Strength in Tension and
- Humidified Deflection

The following points should be noted regarding this testing specification:

- The standard does not address the effect of stress concentrations or penetrations on plasterboard performance
- There is no requirement to understand or calculate the stress-strain behaviour (such as ductility) of the materials
- Rate dependent loading is not considered
- Fatigue performance is not considered
- Bracing strength is not considered
- Robustness/Impact resistance is not considered.

TENSION TEST SETUP

Plasterboard is known to be orthotropic. AS/NZS2588 refers to bending strength tests that must be conducted with plasterboard orientated both parallel to the wrapped edge (or machine direction) and perpendicular to the wrapped edge (or transverse direction). Table 1 of AS/NZS2588 provides minimum bending strength data for various thicknesses of plasterboard. The table indicates that the bending strength in the "perpendicular" direction is in the order of 2.4 times greater than the "parallel" direction. The testing samples used for the tensile strength tests were cut out from 'Standard Core' plasterboard to the following orientations (refer Figure 2 also):

- Longitudinal Direction (= parallel to wrapped edge)
- Transverse Direction (= perpendicular to wrapped edge)
- 45 Degree Orientation

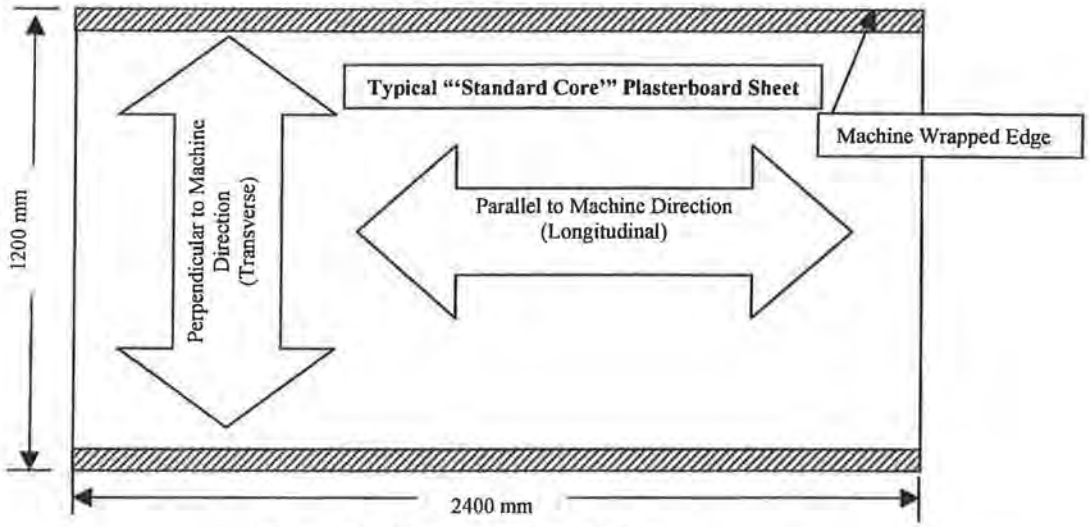

Figure 2 – Plasterboard orientation

Specimens were tested with and without notches cut into the edges. Notches were provided for two reasons. The first reason was to ensure that failure would occur within the gauge length (the length of specimen where displacement was being measured) and the second reason was to estimate the effect that a stress concentration, such as would appear around a window or door opening, might have on the results.

The tension tests were designed to measure the ultimate stress and strain characteristics of the material in all directions. The tests were initially conducted on small "dogbone" shaped specimens but results were not reliable. As a result, the dimensions of the specimen were gradually increased until a reasonable level of repeatability was achieved. The details of the final shape of the specimen are provided in Figure 3.

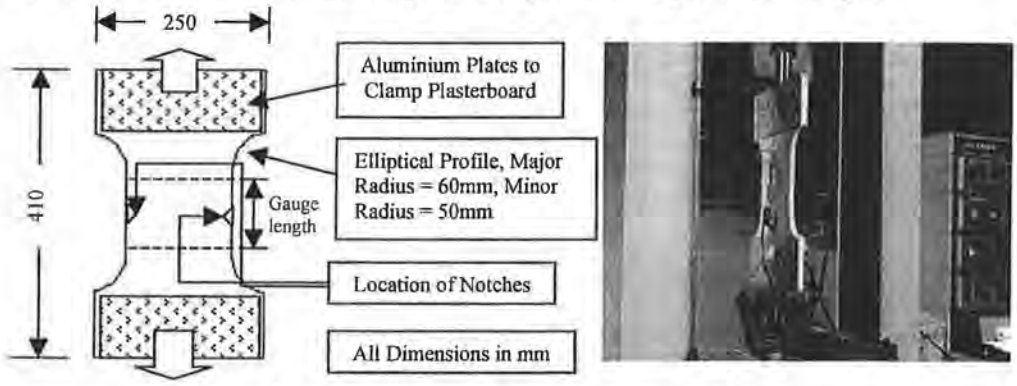

Figure 3 – Final test specimen dimensions and setup

A universal testing machine was used for these tension tests operated in a displacement control mode. Linear Variable Displacement Transducers (LVDT's) were attached to

either side of the specimen using hot glue. The LVDT's measured the total displacement across the gauge length. Checks were carried out to ensure no slip occurred at the clamped ends of the specimen as well as zero bending. Bending was checked by calculating the difference between the two LVDT readings. A loading rate of 0.2 mm/min was applied for each of the tests.

EXPERIMENTAL RESULTS

All specimens were cut from the same batch of 'Standard Core' plasterboard. Test results for specimens with and without notches are presented below.

Specimens without Notches

A total of twelve tension tests were carried out using 'Standard Core' specimens without notches. Tensile stress versus tensile strain curves have been provided in Figures 4 to 6 below and results are summarised in Table 1.

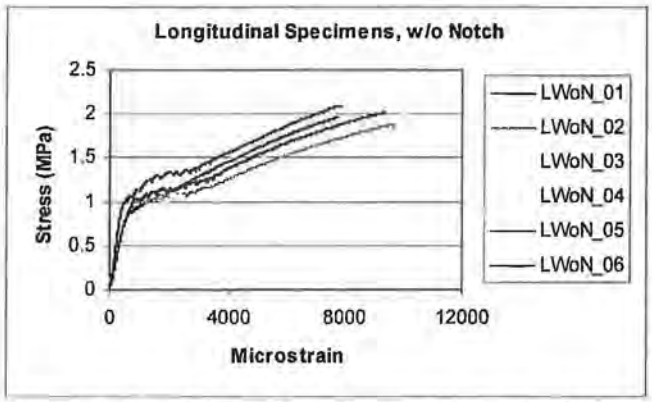

Figure 4 – Longitudinal Specimens without Notches (LWoN_03)

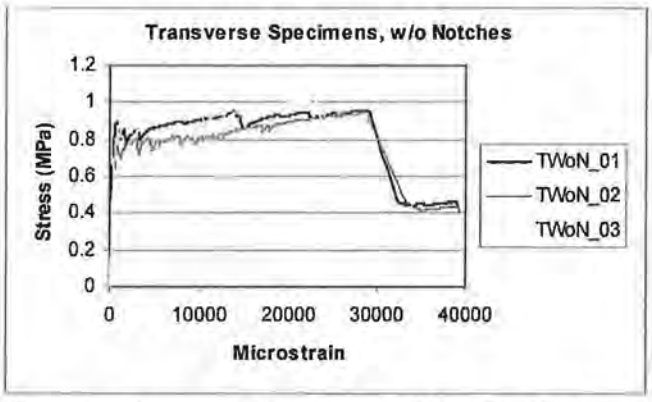

Figure 5 – Transverse Specimens without Notches (TWoN_01)

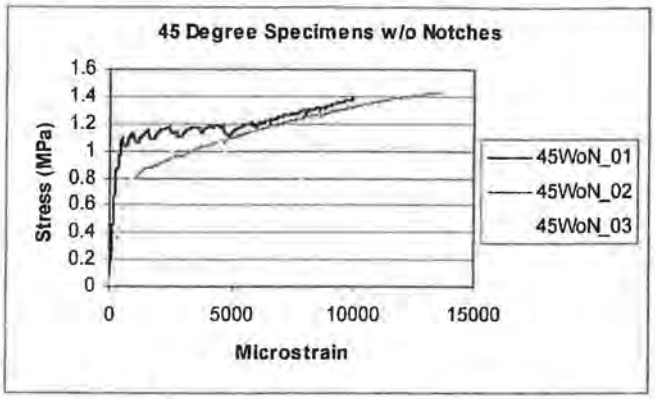

Figure 6 – 45 Degree Specimens without Notches (45WoN_02)

Table 1 – Summary of Test Results for Specimens without Notches

Test Type	Number of Specimens	Ultimate Tensile Stress (MPa)	Coefficient of Variation (%)	Ultimate Tensile Strain (Microstrain)	Coefficient of Variation (%)
Longitudinal	6	2.0	4.2	8,900	11.4
Transverse	3	1.0	3.6	35,200	19.8
45 Degrees	3	1.3	51.2	11,400	51.9

The Coefficient of Variation (COV) is defined as the Standard Deviation for the sample set divided by the Mean and in this case is expressed as a percentage. Longitudinal and transverse specimens without notches exhibited low variability with respect to the ultimate tensile stress, reflected by a COV of just 4.2% and 3.6%, respectively. Ultimate tensile strain however did vary as shown in Table 1. It should also be noted that these specimens (as was the case with the 45 degree specimens) did not always fail within the gauge length of the specimen. This is an important point and is one of the main reasons for conducting notched tests as discussed in the next section.

45 Degree specimens without notches exhibited much higher variability than the longitudinal and transverse specimens without notches. This can possibly be attributed to the random failure plane as illustrated in Figure 6. Regardless of this, the results have shown that the stress and strain properties for a 45 Degree specimen lie somewhere in between the results for longitudinal and transverse specimens. A similar distribution was observed for the notched specimens shown below.

Specimens with Notches

A total of nine tension tests were carried out on specimens with 2 notches. The notches can best be described as small cut-outs with an opening angle of 90 degrees and a depth of approximately 5mm on each side. The location of the notches is shown in Figure 3. Tensile stress was calculated based on a reduced cross-sectional area at the notch. Tensile stress versus tensile strain curves have not been provided for these tests however results are summarised in Table 2.

Notched longitudinal and transverse specimens also exhibited low variability with respect to the ultimate tensile stress, reflected by a low COV of just 3.9% and 2.2%, respectively. Ultimate strain exhibited a slightly better degree of repeatability when compared to specimens without notches. As was expected these specimens always failed within the gauge length of the specimen.

Table 2 – Summary of Test Results for Notched Specimens

Test Type	Number of Specimens	Ultimate Tensile Stress (MPa)	Coefficient of Variation (%)	Ultimate Tensile Strain (Microstrain)	Coefficient of Variation (%)
Longitudinal	3	1.7	3.9	4,800	9.3
Transverse	3	0.94	2.2	15,200	9.5
45 Degrees	3	1.21	3.4	12,100	11.3

The 45 Degree notched specimens exhibited lower variability than the specimens without notches and consistently failed at an angle of approximately 18 degrees to the horizontal.

The results for both sets of specimens have been presented in a "strain corrected" format. The strain correction was deemed necessary due to a small plateau in the stress versus strain curve that occurred in some tests in the very early stages (at <1000 microstrain). The phenomenon that lead to this increase in strain with no corresponding increase in the stress is not yet fully understood and requires further research. The strain correction does not affect the ultimate stress and in all cases is only a small percentage of the ultimate strain. Further, due to the composite construction of plasterboard, the elastic versus plastic parts of these curves are not easily identifiable and as a result Young's Modulus has not been presented. Additional work is currently underway to establish whether the proportional limit in these curves is close to the yield point of the gypsum, the paper or the composite material.

CONCLUSIONS

In domestic residential construction, plasterboard has been traditionally considered to be a non-structural component which provides enclosure to a space with a high quality surface finish. Hence, there is little information available related to the basic material properties. As part of an ongoing investigation into the response of residential structures to low level blast vibrations, it is essential to establish the basic material stress-strain relationship in order to predict the onset of cracking or damage threshold.

Tensions tests have been specifically developed to determine the stress-strain relationship for plasterboard. The tests to date have been conducted on the most commonly used type of plasterboard ('Standard Core'). The tension loads have been applied to specimens along the machine direction, transverse direction and at 45° to the machine direction. The stress-strain curves for each of these loading conditions have been presented. As expected, plasterboard exhibits orthotropic behaviour with a 2 to 1 strength ratio in the "parallel" (machine) direction versus the "perpendicular" direction.

This is primarily attributed to the orientation of the fibres in the paper rather than a characteristic of the gypsum core.

Through testing of notched specimens, it has been found that the effect of stress concentrations can significantly reduce the material's ultimate strength as well as reduce the ductility. Stress concentrators are typically located at the corners of door and window openings in walls. These are typically the locations where cracks start and propagate. Additional testing is currently being carried out to increase statistical significance of the results and also examine other types of plasterboard used in residential structures (e.g. for wet areas).

Static and dynamic racking tests on full-scale walls with openings will be carried out to confirm predictions from analytical models based on the stress-strain relationships established for plasterboard. These wall tests will be used to monitor the onset of cracking and crack propagation in plasterboard under racking loads.

ACKNOWLEDGEMENTS

This research is funded by an ARC Linkage Grant No. LP0211407. The authors would like to acknowledge input and contribution of the research partners Mr. Alan Richards and Adrian Moore of Terrock Pty Ltd.

REFERENCES

Standards Association of Australia, (1998). AS/NZS 2588:1998, Gypsum Plasterboard, Standards Australia

Standards Association of Australia, (1999). AS 1684.2:1999, Residential Timber-Framed Construction, Non-Cyclonic Areas, Standards Australia.

Siskind, D. E., (2000). Vibrations from blasting, published by the International Society of Explosives Engineers (ISEE)

Liew, Y.L., Duffield C.F. and Gad E.F., (2002). The influence of plasterboard clad walls on the structural behaviour of low rise residential buildings, Electronic Journal of Structural Engineering (eJSE), 1, 2002. (http://www.ejse.org).

Moore A.J., Richards A.B., (Terrock Consulting Engineers), Gad E.F., Wilson J.L. (The University of Melbourne), Page A., Fityus S. and Simundic G. (The University of Newcastle), (2002), Report C9040, Structure Response to Blast Vibration, on behalf of the Australian Coal Association Research Program (ACARP).

ASTM C473 (1997), Standard test methods for physical testing of Gypsum Panel Products, American Society for Testing and Materials.

Stagg M.S., Siskind D.E., Stevens M.G. and Dowding C.H., (1984), Effects of repeated blasting on a wood-frame house, United States Department of the Interior, Bureau of Mines Report of Investigations, RI8896

Siskind D.E., Stagg M.S., Kopp J.W. and Dowding C.H., (1980), Structure response and damage produced by ground vibration from surface mine blasting, United States Department of the Interior, Bureau of Mines Report of Investigations, RI8507.